Geomorphology 434 (2023) 108738

Contents lists available at ScienceDirect

Geomorphology

journal homepage: www.journals.elsevier.com/geomorphology

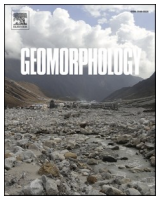

Magnitude of formative flows in stream potholes

J.A. Ortega-Becerril [a], J. Garrote [b,*]

[a] Dpto. de Geología y Geoquímica, Universidad Autónoma de Madrid, Madrid 28049, Spain
[b] Geodynamics, Stratigraphy, and Paleontology Department, Complutense University of Madrid, Madrid 28040, Spain

ARTICLE INFO

Keywords:
Potholes
Formative flows
Spanish Central System
Bedrock channels
2D hydrodynamic model

ABSTRACT

Although it is generally recognized that geomorphic work is tied to bedrock channel reshaping, the importance of low vs. high flow stages that cause the most geomorphic impact remains unclear. The objective of the research is to study the concept of "formative flow" in bedrock channels and determine, through morphological studies, if those flows have any impact on sculpted features such as potholes and how this relationship relates to various inputs such as flow stages (magnitude and frequency), shear stress, and sediment size. Here, we studied the distribution of the main pothole typologies and tried to understand why potholes are found along bedrock river channels. Specifically, we examined stream potholes from three locations along the Spanish Central System: Alberche, Tietar, and Manzanares rivers. We conducted the research by taking precise geometric measurements, classifying potholes, analyzing flow magnitude and frequency, and using a two-dimensional (2D) hydrodynamic model to assess key variables in Manzanares river. This research demonstrated that bankfull depths completely cover all pothole typologies in all the analyzed sites but are not sufficient to achieve its formative flow depth (FFD). Using a detailed 2D hydrodynamic model in Manzanares river, we discovered that dimensions of cylindrical potholes are closely related to bankfull discharge and that this depth is connected to FFD. Other potholes, such as erosive-compound and erosive-lateral, are historical remnants, and their shapes are not related to any particular FFD and are likely associated with rare events and catastrophic breaks. A collection of laterals that exhibit FFD near bankfull flows appear to represent a part of the recent evolution of a knickpoint. To summarize, it can be inferred from the findings that the utility of morphological analysis in conjunction with the 2D hydrodynamic model is to examine the fraction of erosional/active features to determine the degree of senescence and/or change in natural conditions in a river reach.

1. Introduction

Stream potholes are the most common erosive features developed in bedrock channels. Numerous factors contribute to their formation, including flow abrasion through tools called grinders (e.g.,: Charpentier, 1841; Alexander, 1932; Das, 2018), high levels of flow energy expenditure associated with high gradient areas (Goode and Wohl, 2010), weathering (Elston, 1917; Ortega-Becerril et al., 2017), bedrock characteristics (Ortega-Becerril et al., 2017; Ji and Li, 2019), and substrate weakness (Springer et al., 2005, 2006; Ortega et al., 2014). Despite the increase in studies related to pothole formation, limited research has been conducted on the flow stage required to start the erosional processes and the depth that maximizes the erosion over time.

Early publications by Alexander (1932) noted the significance in pothole formation of external processes such as cavitation within eddies and vorticity (Alexander, 1932; Nemec et al., 1982; Jennings, 1983). However, these works largely emphasize the connection between the type of vorticity and the discharge/depth of flow required to start the erosive process. The shear flow entering potholes produces eddies and entrains sediment into depressions, but the question remains: what is the flow depth necessary for sediment entrainment in potholes? Most quantitative studies of pothole geometries have focused on the relationship between depth and radius within individual potholes because these variables affect the development of vortices with vertical axes and hydraulics (Pelletier et al., 2015; Álvarez-Vázquez and De Uña-Álvarez, 2017; Ji et al., 2018, 2019). These variables have been connected to formative mechanisms and internal hydraulics utilizing power functions between pothole depth and aperture size (Kale and Shingade, 1987; Springer et al., 2005, 2006).

The research by Johnson and Whipple (2007) suggests that when potholes are deep enough, there is negative feedback between the rate of expansion and flow dissipation. Pelletier et al. (2015) created a

* Corresponding author.
E-mail address: juliog@ucm.es (J. Garrote).

https://doi.org/10.1016/j.geomorph.2023.108738
Received 18 November 2022; Received in revised form 13 May 2023; Accepted 14 May 2023
Available online 16 May 2023

mechanistic model for eddy-hole pothole formation. The authors of the aforementioned paper highlighted the "lack [of] data-relating pothole size to formative flow depths."

This study aimed to further elucidate the concept of the formative flow depth (FFD) which is the flow depth directly above a pothole. This research is a starting point for several interpretations of the concept (local vs average cross-sectional flow depth, temporal and spatial scale, etc.). Formative flow has been defined as the minimum flow depth needed to start a geomorphic change in a bedrock channel at different scales (Heitmuller et al., 2015). This concept is well known for its role in reshaping the landscape during high-magnitude floods (Baker and Kale, 1998; Venditti et al., 2017); however, its relationship to small-scale features such as pothole erosion is not widely studied (Pelletier et al., 2015). The formative processes (Nemec et al., 1982) involve flow separation that causes boulder-induced bedrock erosion, macroturbulence (e.g., in river banks, Lorenc and Saavedra, 1980), and the likelihood that there is a critical scour depth (Nemec et al., 1982). The two-dimensional (2D) nature of turbulence is represented by potholes, which may be related to flow depth and other factors (Zen and Prestegaard, 1994). When a stream pothole reach their mature state, the depth is greater than the diameter; hence, the diameter and depth relation (D/h) serves as a gauge for hydraulic power (Ji et al., 2018). In channels with a gradient of 0.1 m/m, Pelletier et al. (2015) discovered that the flow depth required to create potholes is nearly equal to the diameter of the pothole. This idea is strongly related to that of "geomorphic work" (Wolman and Miller, 1960), which states that moderate flows that occur frequently have the highest geomorphic impact. This is because the greater magnitude-frequency products accomplish more geomorphic work than less powerful ones but instead they have more magnitude-frequency flows.

The objective of this research is to test the role of low-magnitude flows in pothole development and to establish whether different pothole typologies are located and distributed along any specific areas affected by erosional processes and, consequently, by certain discharges (formative flows) and flow depths (FFD).

Once we surveyed the range of pothole morphologies and its FFD, questions arose on the frequency of those depths and the required flow discharge for starting the erosional process. A large portion of work is done by events of moderate magnitude in alluvial rivers (Wolman and Miller, 1960), but it is well known that large valley scours and substantial boulder movements require events of high magnitude. However, during such occasional flows, ordinary small-scale potholes have been reported to be breached and removed, and large-scale potholes have been formed (e.g., Baker, 1973; Baker and Kale, 1998; Bera et al., 2019).

We classify every pothole into morphotypes and determine its distribution in bedrock river channels as well as how these factors relate to other factors such as flow stages, shear stress, and sediment size. To determine whether different discharges may be associated with a particular pothole (feature, degree of maturity, position, and size), we employing actual flood events and comparing the various flow depths with FFD and morphometric measurements of potholes. Moreover, we explore how stream potholes might be used as morphologic indicators of average flow conditions in natural regimes and possibly of relict conditions in the context of human-modified basins. Paying attention to the regularity with which certain flow depths are reached may enable us to identify the types of potholes that are being covered by waters and to determine what may be the current active erosion process (if applicable) at each location.

In order to improve our understanding of the flow conditions under which potholes are formed, we measured the size (diameter, depth) of the major potholes along three sites of the Spanish Central System (Ortega et al., 2014), two of which (Tietar and Alberche rivers) were continuously measured and the third (Manzanares river) ungauged. By conducting fieldwork during and after floods, we recorded flow depths in proportion to discharge (in gauged sites) at various pothole groups according to its typology and performed a 2D hydrodynamic model in the ungauged site using a detailed Digital Elevation Model (DEM) (Gomez-Heras et al., 2019).

1.1. Study area and geological background

The study area is situated in the central Iberian Peninsula along the Spanish Central System, a mountain range that runs across the Iberian Peninsula from SW to NE (Fig. 1). The mountain range is formed with Paleozoic-age crystalline rocks, mostly granites and gneisses. We studied bedrock outcrops at three study sites: the Tietar (TM), Alberche (AB), and Manzanares (MCV) rivers. Specifically, we studied porphyric biotitic monzogranite outcrops at Tietar, porphyric leucogranite outcrops at Alberche, and coarse-grained leucogranite with interbedded microdiorite dike outcrops at Manzanares. Dikes exert strong lithologic control.

We performed the research at three sites located in bedrock reaches in the headwaters of the Tietar, Alberche, and Manzanares tributaries of the Tagus, one of the major rivers of the Iberian Peninsula. The three rivers are situated in the piedmont of the mountain range, with the annual precipitation ranging from 700 to 900 mm. Floods occur in winter because of frontal systems and snowmelt in the late winter/spring, particularly in the Alberche river. However, powerful storms with flashflood characteristics are frequent during autumn in Tietar and Manzanares. Table 1 summarizes the key features of the study sites. Large floods in the region can exceed the annual peak discharge at some locations by six to eight times (Ortega et al., 2014). The geomorphological surroundings vary from one site to the other. The Tietar site exhibits a high gradient reach (0.025 m/m) with boulders and rapids, and the river passes three rocky outcrops where the local gradient increases up to 0.05 m/m. The Alberche has a gradient that is comparable to Tietar's (0.027 m/m), and the reach shows rapids along a bedrock bench that is more resistant to erosion where the gradient is 0.05 m/m and where most of the potholes are located. The Manzanares has a segment with a higher gradient (0.12 m/m) and a knickpoint with a gradient of 0.2 m/m. Although boulders are present along the whole run, the sediment transported during the floods is coarse, consisting of gravel bedload from Alberche and Tietar rivers and gravel-boulders from Manzanares river with more exposed bedrock.

1.2. Pothole morphotypes and evolutive stage

There are various pothole morphotypes depending on their morphology, level of flow activity and evolutionary maturity (e.g.: Alexander, 1932; Nemec et al., 1982; Kale and Shingade, 1987; Lorenc et al., 1994; Richardson and Carling, 2005; Singtuen and Junjuer, 2021). Alexander (1932) classified potholes into three categories: eddy holes (cylindrical) created by abrasion by swirling currents, gouge holes (open, U-shaped like grooves) formed by lateral flow impact, and plunge-pool holes formed by falling flows. Sato et al. (1987) described another type: the "half potholes" which are similar to the "lateral potholes" described by Zen and Prestegaard (1994). These features are open depressions that have been influenced by plucking and are marginally situated on river margins. Sato et al. (1987) described the aforementioned typologies and a "compound" one, an irregular depression. Thus, questions arise as to what each form of stream pothole represents in terms of the evolution, maturity, and current active growth of stream potholes.

Nemec et al. (1982) divide potholes according its degree of development as follows: young stage (low maturity, symmetrical depressions), cylindrical (symmetrical, active potholes), and asymmetrical bulgy (old stage, high maturity), which exceed a threshold that limits the lifting of particles out of pothole. Lorenc et al. (1994) developed a pothole evolution route from early-stage scour holes to late-stage "bulbous and irregular holes" based on their field observations. Álvarez-Vázquez and De Uña-Álvarez (2017) identified similar categories, suggesting morphological thresholds that distinguish between

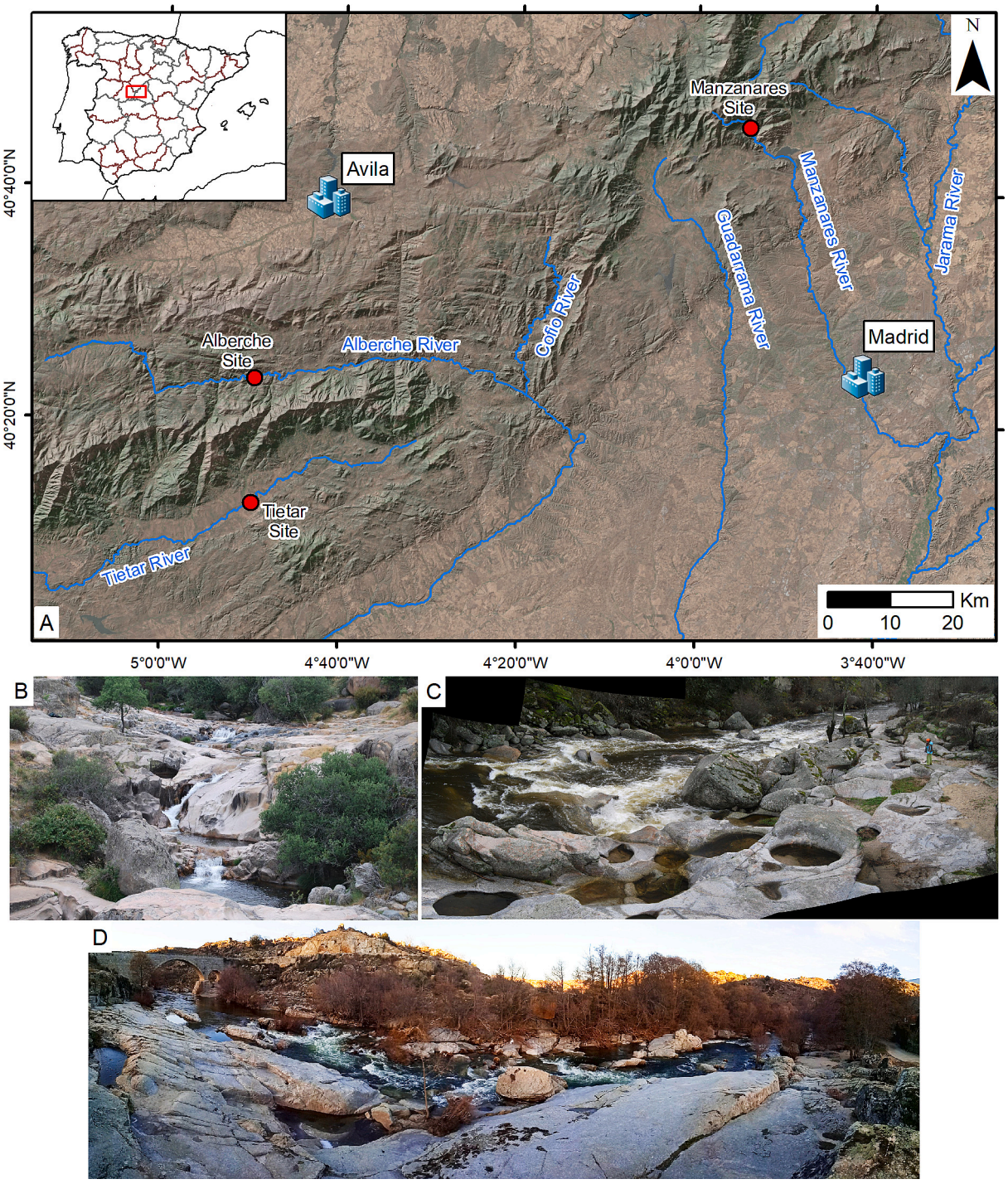

Fig. 1. Study area with the three sites along the Spanish Central System.

active growth from inherited (stationary growth) forms. Richardson and Carling (2005) differentiate three growth stages: (i) initial (smooth cavities), (ii) intermediate (deeper cavities) and (iii) advanced (coalescent, inner channel connects single forms).

The development of potholes may also be related to their position along the channel and the geometry of the same (Kanhaiya et al., 2019). In experimental designs, Johnson and Whipple (2007) noted that potholes on a 0.07 % slope can be inherited forms. However, in general, the potholes developed in the modern streambed are considered contemporary (Wang et al., 2009).

Conditions can be interpreted as mature once the evolution ceases, i.e., when changes are no longer occurring or when they occur at a slow rate of erosion. (e.g., the evolution of the channel may lead to the rapid development of a strong incision and potholes cannot fully develop, Wang et al., 2009); moreover, the feature can be eroded, and the depth of a pothole may be reduced by a vertical incision (Springer et al., 2005). In terms of the pothole evolution, although the process of the formation of potholes is always erosive, we have considered two stages: (1) constructive phases that take place during early to intermediate stages where single forms evolve with deepening and widening, and (2) destructive phases during the advanced stage with secondary sculpting, breaching of floor/walls, and the development of compound and lateral potholes.

In total, we recorded potholes along three sites (Table 1 and

Table 1
Main characteristics of the studied sites.

	Catchment		
	Tietar	Alberche	Manzanares
Drainage area[a] (km^2)	301	480	50
Q_2 ($m^3\ s^{-1}$)	82	157	24
Bankful discharge ($m^3\ s^{-1}$)	129	262	37
Q_{500} ($m^3\ s^{-1}$)	543	1213	145
Flow regime (Q_{500}/Q_2, $m^3\ s^{-1}$)	6.6	7.7	6
2018 flood ($m^3\ s^{-1}$)	160	308	Ungauged
2019 flood ($m^3\ s^{-1}$)	218	308	Ungauged
Basic morphology	Rapids	Rapids	Knickpoint
Gradient (m/m)	0.025 (0.05[b])	0.027 (0.05[b])	0.1 (0,2[b])
Channel width (m)	11–18	6–13.9	4.6–12
Sediment transport (max. size)	Gravels	Gravels	Boulders[c]
# potholes studied	45	77	60
Pothole area (m^2)	2840	8331	2346
Pothole density (potholes/km^2)	0.015	0.009	0.025
# joints and orientation	122 (NW, NE)	121 (ENE, WNW)	86 (N, E, NW)
Joint density (joints/km^2)	42.95	14.52	0.03

[a] Drainage area upstream of the study site.
[b] Gradient at rapid/knickpoint.
[c] Sediment size (D_{50}) inside the potholes is listed in Supplementary material.

supplementary material) and categorized them visually into four groups during fieldwork (Fig. 2).

1) Incipient (Fig. 2A): shallow bedrock depressions with polished smooth walls that often have no sediment infill (Richardson and Carling, 2005). Nemec et al. (1982) and Lorenc et al. (1994) claimed that it indicates low maturity, as did Richardson and Carling (2005), who mentioned their near-circular shape as an indicator of early stages of pothole development; however, as these forms have been intensely conditioned by weathering, it is also possible that such forms developed under mature conditions of a reach.

2) Cylindrical (Fig. 2B,C): simple, circular potholes (Richardson and Carling, 2005), described by Nemec et al. (1982) as symmetrical and active potholes that use a vortex with vertical axes to concentrate the flow energy and erode the bedrock ground. The mobile erosion nodes may evolve into stationary ones that develops into cylindrical cavities (Springer et al., 2005). Sato et al. (1987) observed these features along reaches with gradients between 0.1 and 0.4 m/m. Pelletier et al. (2015) considered their morphology and dimensions optimal for growth. Knickzone potholes are a type of these potholes. These potholes, which are situated at the knickpoint upper lip and rapids, involve considerable flow energy concentration and erosion. Although a reduced flow depth is expected due to critical flow, these potholes function similar to cylindrical ones. This is in line with Thompson's (1990) observations that vertical potholes are concentrated near knickpoints because of gradient steepening, increase in velocity, and decrease in flow depth. We will consider both types within the same category. Wang et al. (2009) identified the preservation of a cylindrical shape in some abandoned potholes; thus, they can sometimes be considered senile features. Recent upstream migration of a knickpoint may leave potholes with a near-cylindrical shape.

3) Lateral potholes (Fig. 2E): rounded depressions in channel sidewalls, sometimes with a closed depression and sometimes with an open floor (Richardson and Carling, 2005), located on river banks and/or flanks of channel islands, generally in groups strung out on the outcrop and facing downstream within the shear zones and flanks of obstacles (Zen and Prestegaard, 1994). Owing to their breached condition, lateral potholes suggest flow separation, erosion in the bedrock borders, and a certain degree of maturity. These features have also been recommended as an efficient mechanism for modifying bedrock channel width (Lorenc and Saavedra, 1980; Zen and Prestegaard, 1994). Richardson and Carling (2005) classify these features into six types.

4) Compound (Fig. 2F): open, coalesced, and breached potholes signaling advanced development. When the depth and diameter increase, single potholes evolve to compound and coalescing morphologies (Álvarez-Vázquez and De Uña-Álvarez, 2017). Kale and Shingade (1987) reported that coalesced potholes frequently occur around the center of the channel, and Richardson and Carling (2005) mentioned the connection of single forms by an inner channel and the development of compound forms. The coalescing complex forms with secondary sculpting support the idea of different stages of development occurring simultaneously (Álvarez-Vázquez and De Uña-Álvarez, 2017).

2. Materials and methods

To achieve our objectives, we propose the following analysis: (1) record the main geometric measurements of potholes along the tree studied sites, (2) classify each of the potholes into one of the four morphotypes, (3) obtain the water depths reached by flood waters in the two gauged sites (Alberche and Tietar rivers), (4) calculate the FFD in potholes, (5) perform 2D hydrodynamic modeling of the ungauged site (Manzanares river), and (6) estimate the discharge that fits better with the FFD of every morphotype.

2.1. Field measurements

Approximately 180 potholes were selected for systematic field study that included taking geometric tape measurements such as depth and diameter. To obtain accurate depth readings, grinders were removed from filled potholes. We also calculated the relative mean height in each pothole, the difference between the mean water depth, considered in the adjacent channel, perpendicular to the main flow direction at arbitrary flow depth, and the pothole center elevation. In lateral and coalesced potholes, we recorded the highest elevation at the sculpted surface. Pothole heights were determined from the water depth using a laser rangefinder.

In our field work, we placed each pothole into one of four categories according to the four types of potholes generally accepted by researchers (e.g., Nemec et al., 1982; Kale and Shingade, 1987; Sato et al., 1987; Zen and Prestegaard, 1994; Richardson and Carling, 2005; Ortega et al., 2014; Yin et al., 2016): incipient, cylindrical, lateral, and compound. According to the aforementioned authors' description and using qualitative sorting, the classification was made visually (Fig. 2).

Pictures were taken to record two river floods (in 2018 and 2019), both of which covered bedrock outcrops. The flow discharge was measured at each stage using the automatic flood warning system of the Tagus basin with a 15 min interval at the Alberche and Tietar sites. The Manzanares river is ungauged.

2.2. FFD calculation

To estimate the formative flow, we used the method proposed by Pelletier et al. (2015), using the pothole axis and depth measurements to check the aspect ratio (γ), a parameter independent of the spatial scale that relates the pothole depth (Z) and radius (R) (Eq. (1)):

$$\gamma = Z/R \quad (1)$$

To analyze circularity (a measurement of cylindrical shape), we plotted the maximum vs. minimum axis. The level of activity of the reach may be known to us through this analysis. We consider the more active ones circular potholes, according with Nemec et al., 1982; Álvarez-Vázquez and De Uña-Álvarez, 2017, whereas elongated, convoluted, or irregular potholes can be a sign of incipient or relict conditions (Sato et al., 1987; Lorenc et al., 1994).

To calculate FFD, according to Pelletier et al. (2015), we use Eq. (2):

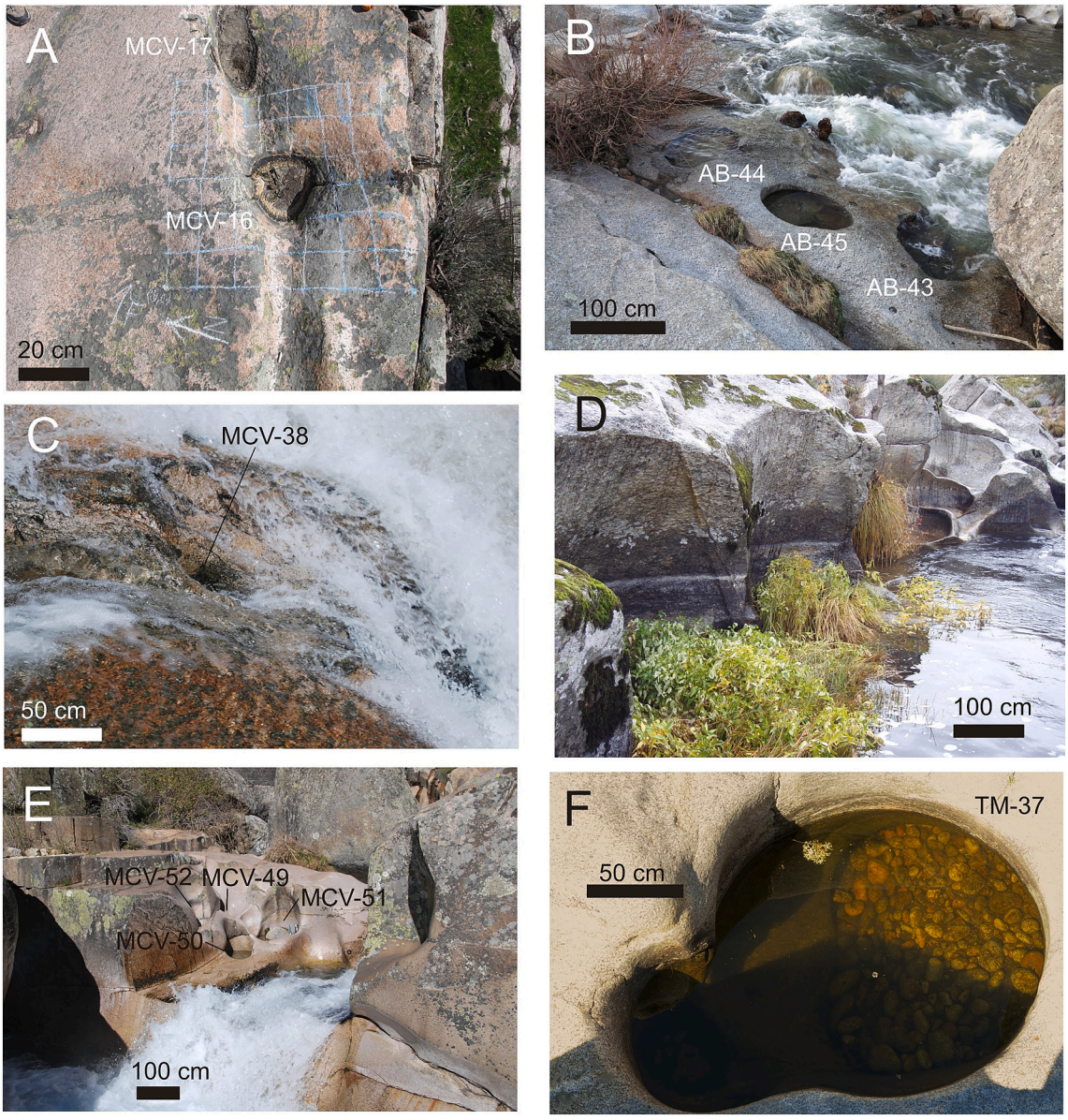

Fig. 2. Types of potholes in the study area. A. Set of incipient depressions connected by a runnel (Manzanares), B. Set of cylindrical potholes in the active channel (Alberche river), C. Knickzone and cylindrical pothole during a low flood stage (Manzanares river), D, E. Lateral (Manzanares, Alberche), F. Compound pothole in an inner channel (Tietar river).

$$0.23\frac{R}{S} < FFD < 2.2\frac{R}{S} \quad (2)$$

where *FFD* describe a range of flow depth values, *R* is the pothole radius, and *S* is the channel gradient.

From their dimensions, we calculated the FFD at each pothole and compared it with flow depth at various flow discharges. Our hypothesis is that cylindrical potholes at the current knickpoint must be the best fit between the hydrodynamic model and FFD for the current "active potholes," which are cylindrical.

2.3. 2D hydrodynamic model

At the Manzanares site, hydraulic river flow simulation was performed using the 2D hydrodynamic model software Iber (Bladé et al., 2014). Iber is a 2D numerical model that simulates free surface flow in rivers by resolving 2D Saint-Venant equations. To determine the depth of the water and the two components of the depth-averaged velocity at the XY plane, Iber software solves the full depth-averaged shallow water equations. These equations are solved using unstructured meshes and explicit finite volume techniques.

The high-resolution topography used in the hydrodynamic models was created using a regular mesh with a resolution of 5 cm and was acquired from UAV photogrammetry (Gomez-Heras et al., 2019). However, to have a realistic mesh structure, the spatial resolution of the Iber 3D mesh must be decreased to 0.4 m. Thus, the 3D mesh accuracy on Z values shows a mean error lower than 0.1 m. The positions of the inflow and outflow were chosen to define a critical flow regime. The Iber model's flow regime properties are partly responsible for this hydrodynamic simulation setup. The roughness coefficient (Manning's value), another important factor in the construction of the Iber model, was obtained via field work and high-spatial-resolution ortho-images generated using UAV photogrammetry, employing previously proposed Manning's values such as those of Arcement and Schneider (1989) and Chow (1959); in this case, Manning's values in the range of 0.03–0.05 were used as the basis for the different effects of surface irregularities.

Peak flow measurements connected to different return period frequencies, ranging from a 2-year return period to a 50-year return period, were used in the 2D hydrodynamic analysis (including the bankfull stage, which is close to the 5-year return period at the study site). Up to ten peak flow values (5, 7, 8, 10, 15, 22, 24 (Q_2), 37 (Bankfull, Q_5), 54 (Q_{10}), and 72 (Q_{25}) $m^3\ s^{-1}$) were used for the hydrodynamic models. Taking into account the Iberian Peninsula climatology, the bankfull stage is not just related to the ~2-year return period (as it could be related in a global worldwide approach, e.g. Leopold, 1994), but spans from a 2-year return period in the northern area to a 7-year return period in the south (which is well correlated with previous results as Williams, 1978; Mosley, 1981; or Sherwood and Huitger, 2005). Within the study area, the bankfull stage is related to the 5-year return period peak flow. Because the Manzanares basin is ungauged until far downstream, the peak flow data used for hydrodynamic analysis were obtained using the CauMAX software, a free program developed by the Spanish Minister of Ecological Transition, following Jiménez Álvarez et al. (2013).

The results for each simulation were obtained and exported into georeferenced raster format (ASCII raster) with a spatial resolution of 0.1 m. These results concerned flow depth, flow velocity, bed shear stress, and critical diameter. The location of the potholes (extracted from the high spatial resolution ortho-image) was used to extract hydraulic characteristics such as flow depth and shear stress from the exported raster files after interpolating from the 3D mesh nodes using the nearest neighbor method and importing them into a GIS environment.

To estimate FFD from hydrodynamic model results, we used the Rouse number (Eq. (4)) as a method to determine if the flow can entrain sediment from potholes and is, therefore, effective work.

$$Ro = \frac{w_s}{Ku_*} \propto \frac{w_s}{u^*} \tag{4}$$

Here, w_s is the particle settling velocity (a function of particle size and density), K = 0.41 is von Karmen's constant, and $u^* = (\tau/\rho)^{1/2}$ is the shear velocity (τ is shear stress and ρ is fluid density). According to Julien (1998), when R is >7.5, the flow is unable to entrain sediment from the bottom of the pothole, which causes pothole formation to slow down or cease entirely.

Further, we assumed that grains are in suspension when $u^*/w_s > 1$ because u^* scales with fluid turbulence and can act as a vertical force to suspend grains, while the settling velocity measures how quickly gravity returns particles to the bed. The empirical formulas of Ferguson and Church (2004) can be used to estimate the value of the w_s, which is dependent on grain size. For particle diameters significantly $>10^{-3}$ m, this means that the settling velocity in water is approximately equal to 4.65 times the square root of the grain diameter (m). Since estimating u^*/w_s in specific potholes is challenging, it seems reasonable to assume that shear stresses at the base of the pothole will be lower than the shear stresses on the river bed in places without potholes. Thus, if $u^*/w_s < 1$ (or Ro is >7.5) in the main channel (around the pothole location), then potholes will not likely be able to suspend grains.

The Rouse number depends on grain size since the w_s are used in its calculation. Our analysis considered two different particle grain sizes (D_{50} and Pothole radius) because the determination of the Rouse number is complicated by the variability of grain size. When particle grain size is equal to the radius of the pothole, we assumed that the river flow can entrain all of the sediment from the pothole and move them as bed loads, allowing the pothole to develop more rapidly.

3. Results

To better understand the role of potholes in the evolution of bedrock rivers, their morphology, and the flows that maximize bedrock erosion — the formative flows — we analyze the following: (1) Different pothole morphologies and FFD based on geometrical parameters, (2) flow discharge and its relationship with FFD and pothole location in gauged basins, and (3) the use of hydrodynamic 2D modeling to understand FFD in ungauged basins.

3.1. Pothole morphology and formative flows based on their geometry

As shown in Fig. 3 (panel in Fig. 1B to D), the three sites studied display various patterns in the histogram of pothole typologies. In Tietar river, there are a few cylindrical potholes, which are mostly associated with inner channel development (pothole TM-37, Fig. 2F) and downstream boulder obstruction (pothole TM-39). These would suggest poor bedrock erosion and low activity in terms of pothole formation in the current stream. Furthermore, the abundance of erosive compound potholes, which are the remains of previous conditions, indicates that the reach is in a relict stage. As defined by Sato et al. (1987), potholes in this area could be categorized as fossil potholes. Lateral potholes are located along the three bedrock prows and show the channel widening. The absence of cylindrical-knickzone potholes could be attributed to the presence of low gradients. Pothole morphologies in this reach may indicate a nearly complete former-knickpoint erosion.

Alberche river exhibits several cylindrical potholes that are closely associated with the local steepness of bedrock ground. Due to the homogeneous/massive nature of bedrock (Ortega-Becerril et al., 2017) and the absence of widely spaced jointed blocks, aside from horizontal jointing, incipient potholes are essentially nonexistent on the site. This feature could encourage the existence of vertical vortexes and cylindrical potholes (Ortega et al., 2014). The high number of cylindrical and lateral potholes may also indicate (i) an extremely active reach, despite the knickpoint end, or (ii) remnants of past active potholes because most cylindrical potholes have small depths in comparison with their diameter. This may imply the removal of the upper half by the plucking erosion of bedrock ground due to the occurrence of horizontal jointing. The last hypothesis sufficiently explains the abundance of erosional groupings of potholes (erosive-compound and erosive-lateral).

The Manzanares river site is a step-pool reach with several knickpoints and exhibits a typical sequence of early-stage potholed reach features, including a substantial number of lateral potholes downstream of the main knickpoint, cylindrical and plucking-elongated potholes on the knickpoint lip, and incipient potholes upstream the waterfall. From downstream to upstream, there is a notable decrease in maturity in the pothole morphology, and this distribution correlates well with the upward migration of knickpoints.

By conducting a field survey, we recorded and plotted in a loglog diagram the axis dimension (max vs. min) of every pothole along the three studied reaches (Fig. 4) to obtain circularity, a characteristic trait of eddy-hole-type potholes (cylindrical). Manzanares has the best fit (R^2 = 0.91) with less dispersion of results and is closest to a 1:1 line (the highest degree of circularity), whereas the Alberche and Tietar sites show R^2 values of 0.70 and 0.68, respectively. These values are consistent with our field observations, showing that Manzanares is the more active knickpoint zone, while Alberche and Tietar exhibit a rapid landscape.

According to Pelletier et al. (2015), there is a linear relationship with a most common depth-to-radius or aspect ratio of 2. Over the entire range of scales at which potholes occur, plotted aspect ratios are roughly proportionate. However, from Fig. 5, we obtain a difference in behavior in Tietar river with shallower potholes. This is consistent with the abundance of coalescent and breached potholes. Manzanares and Alberche follow a “normal” pattern. At the Manzanares site, the two types of lithology (microdiorites and leucogranites) lead to a changing pattern in terms of the aspect ratio, as illustrated in Fig. 5B. Granitic potholes complement better with other granitic areas such as the Alberche site.

We calculate the minimum flow depth required for pothole formation (Eq. (2)) along the three studied sites by first considering all pothole data and, second, only on the basis of cylindrical, active potholes. Fig. 6 shows the FFD of the three sites, which was calculated using all the

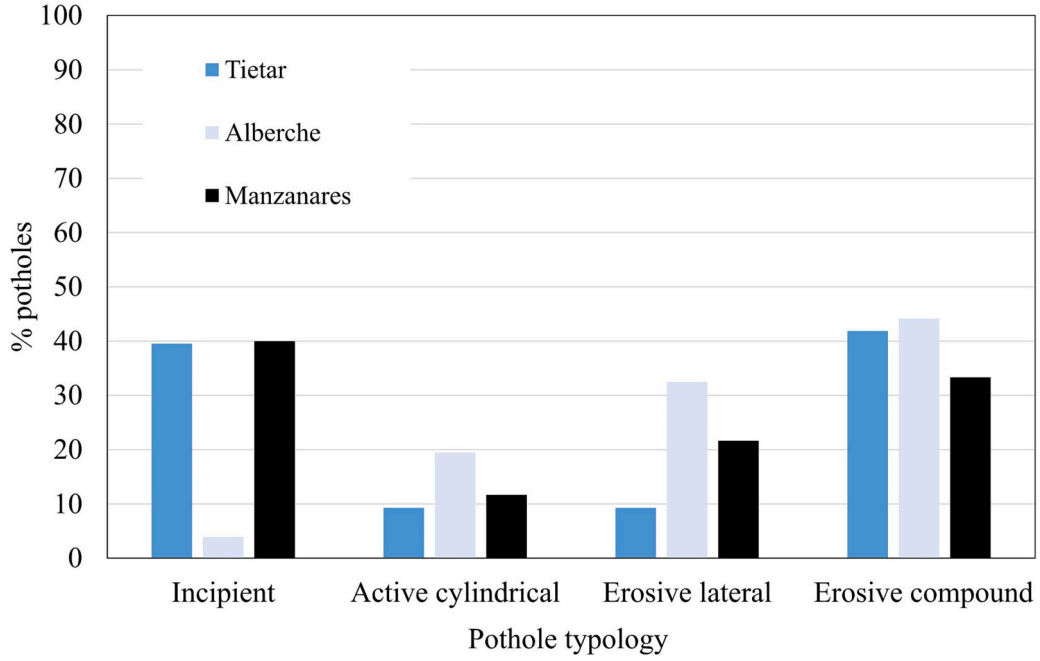

Fig. 3. Histogram showing the distribution of pothole types in the three studied sites.

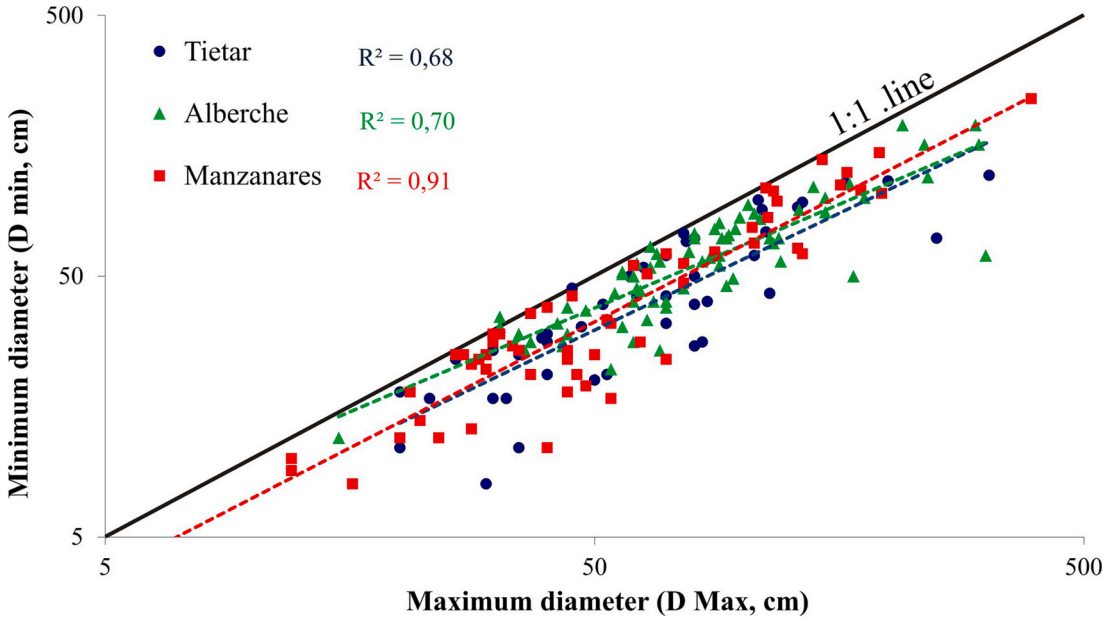

Fig. 4. Circularity of the three studied reaches.

potholes. Due to the inclusion of erosive-compound and incipient potholes, with high/low diameter values, formative flow depths considering all the potholes show a considerable dispersion of results, which is greater in Tietar and Alberche rivers than in Manzanares. We believe that this result does not accurately reflect the effective flow depth required for pothole work. In addition, field observations suggest that most of the erosion comes from the plucking process.

Conversely, calculations based only on cylindrical potholes (Fig. 6) are accurate and constrain the FFD at ~60 cm in Manzanares and ~ 3 m in Tietar, with variable measurements (2.3–3.8 m) in Alberche. The results are limited by the low number of cylindrical potholes in Tietar (N = 4) and Manzanares (N = 7), which are only present along the active channel (Tietar) or knickpoint lip (Manzanares). Alberche (N = 16) has a greater number of cylindrical potholes, but statistical variables (see Table 2) shows greater variability. We interpret this diversity as the result of studying all the cylindrical potholes collectively despite most of them are remnants.

Because most features under "mature conditions" reflect pothole diameters larger than the "present flow" that maximizes bedrock erosion, the FFD in reaches with considerable pothole variability must be carefully analyzed. Tietar has high variability in potholes and mature conditions, and Manzanares still has an active knickpoint and more accurate results. We interpret the results as the response of different evolutionary stages of bedrock rivers; greater compound erosional forms are observed at lower heights and more incipient depressions at higher levels. The strong lithologic control of the microdiorite dikes upstream

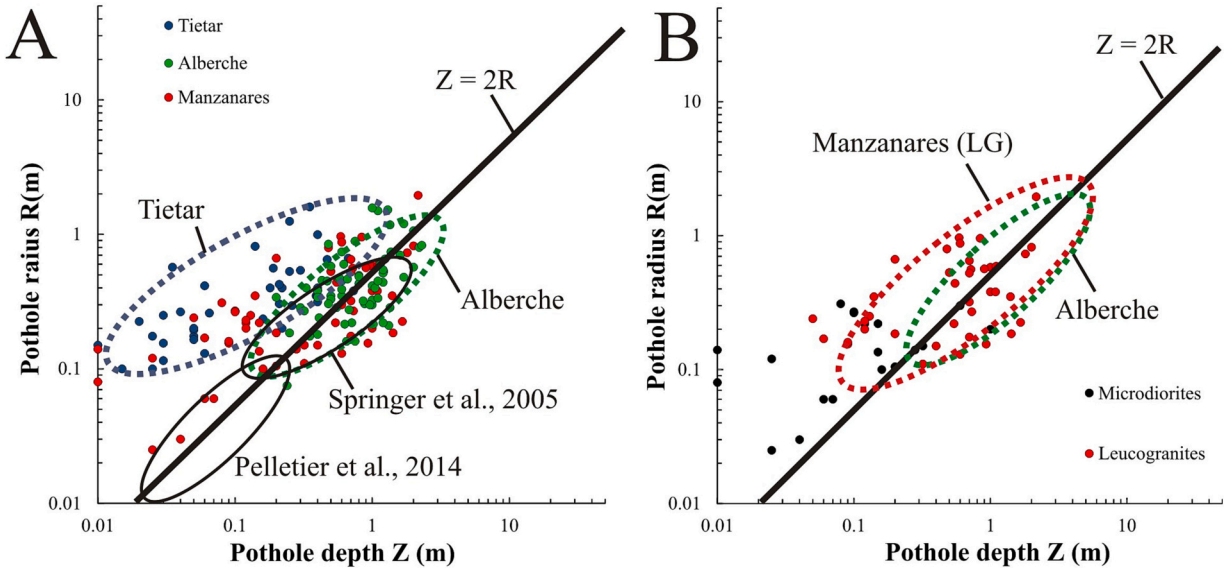

Fig. 5. Plot of the relationship between the depth and radius of bedrock channel potholes. For each investigated reach, dashed ellipses display the general range of data values; solid ellipses indicate data from Springer et al. (2005) and Pelletier et al. (2015). The solid black line corresponds to $\gamma = Z/R = 2$. A. All studied reaches and results from other works. B. Results for Manzanares and Alberche. Note: in Manzanares, there are two types of lithologies: microdiorites (black dots) and leucogranites (red dots).

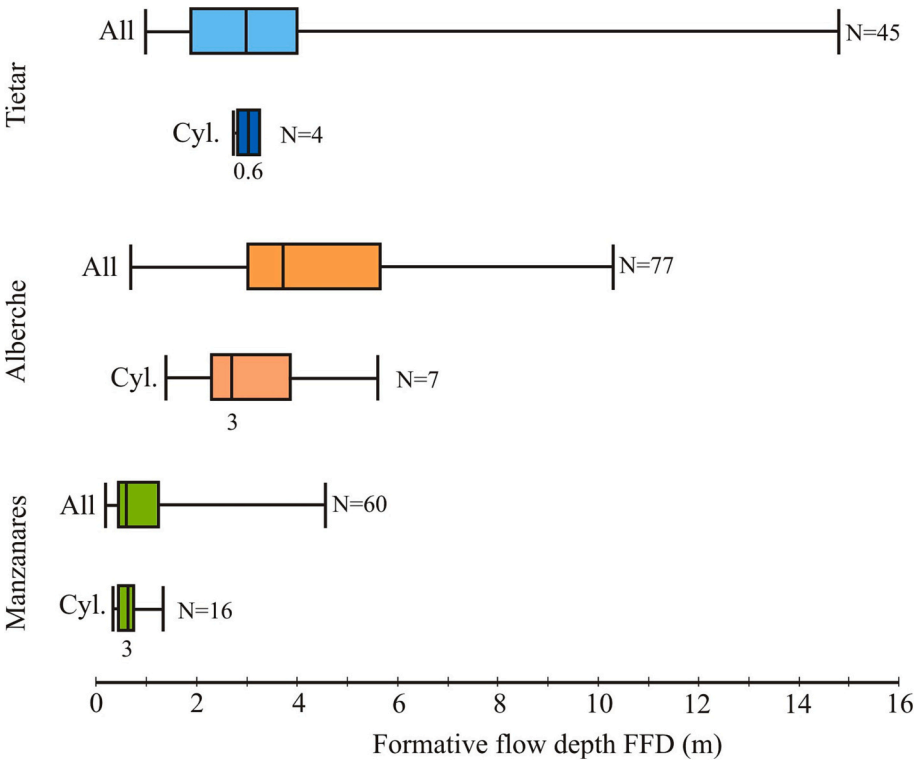

Fig. 6. Box plots of formative flow depth (FFD) along the three sites, including all potholes and cylindrical ones only.

of the knickpoint in the Manzanares site may also be the cause of the different results (see Fig. 5B). For better accuracy regarding flow hydraulics and FFD, cylindrical features may constitute the best pothole typology.

3.2. Flood discharge in Alberche and Tietar gauge stations: flow depths that reach pothole levels

In recent years, the two gauged reaches, Alberche and Tietar, witnessed a string of low-magnitude floods that were nearly at the bankfull stage. Both rivers are part of the automatic flood warning system of the Tagus basin (SAIH). The system contains online discharge data.

We were able to visit both sites during flood events and during several levels of flood hydrograph situations. By continuously monitoring the 2018 and 2019 flood flows in the gauge stations and the water depths that those discharges reached at the sites (Table 1, see Figs. 7 and 8), we obtained the minimum discharge necessary to reach and cover the

Table 2
Statistical results of minimum formative flow depths (in m) according to pothole radius and gradient in the studied sites considering all potholes and only cylindrical potholes.

	Tietar		Alberche		Manzanares	
	all	cylindrical	all	cylindrical	all	cylindrical
Min	0.9	2.7	0.6	1.4	0.1	0.3
Max	14.7	3.2	10.2	5.6	4.5	1.3
Mean	3.6	3	4.1	3	0.8	0.6
SD	2.9	0.3	2.7	1.2	0.7	0.3
CV (%)	78.4	9	65.9	38.8	92.8	52.4

potholes, but those depths may not have sufficient water to reach the FFD in all groups of potholes.

(1) Channel active potholes (~6 $m^3 s^{-1}$ in both rivers).

(2) Strath terrace and compound potholes (~20 $m^3 s^{-1}$ in Tietar and ~ 30 $m^3 s^{-1}$ in Alberche). This depth is similar to the requirements to cover rapid bedrocks in Alberche river.

(3) The water depth at which all potholes of the studied section are covered by flood waters (~40 $m^3 s^{-1}$ in Tietar, estimated, not observed, and ~60 $m^3 s^{-1}$ in Alberche). This depth is capable of covering lateral potholes at the top of the sculpted end and assumes a lower depth than the Q_2 flow.

(4) All bedrock section are covered by water (~90 $m^3 s^{-1}$)

(5) Maximum flood depth (~218 $m^3 s^{-1}$ in Tietar and ~308 $m^3 s^{-1}$ in Alberche). Unfortunately, because the floods occurred at night, we were unable to document the peak discharge depths at either site with photographs or measurements. Thus, we used flotsam on river banks to accurately determine the maximum depth.

Most of the potholes are covered by the bankfull discharge. Flow depths and pictures taken during several flood events are shown in Figs. 9 and 10.

The spatial occurrence of potholes is compared with the bed elevation concerning some arbitrary water surface elevation, which connects the pothole to the local hydraulics. In Fig. 11, we plotted the elevation of cylindrical potholes in the Alberche site, the calculated FFD, and the highest point of the well-known 2019 flood (210–230 cm over the rapids, 275 cm over active potholes, 210 cm over strath terrace 210 cm and 0.15 cm in top of highest lateral potholes). Although all the surveyed potholes were covered by water, not all of them reached their FFD. Major deviations occur along channel obstructions, such as in the big boulder area where flow is locally affected. Another important question arises regarding the "real activity" of all potholes. Some of the greatest divergences are associated with cylindrical but truncated potholes that clearly form part of the relict bedrock level.

3.3. FFD and 2D-hydrodynamic modeling in the Manzanares site

The hydraulic river flow simulation at the Manzanares river, using a fully 2D hydrodynamic model, allows us to ascertain the flow depth at each pothole for different peak discharge scenarios and compare this flow depth value with the calculated FFD.

The results of the 2D hydrodynamic modeling at the Manzanares site have revealed a strong relationship between two variables: peak flow depth value and surface topography. Therefore, these two variables have a significant impact on the form and spatial distribution of flow depth values. Surface topography in the studied Manzanares R. reach shows multiple stepping forms, obstacles in the way of water flow, and surface depressions or sinks.

All these surface patterns appear to be to some extent regulating the water flow of the Manzanares and producing variations in both flow depth and flow pattern morphology. As is shown in Fig. 12, for lower peak flows (i.e., 10 $m^3 s^{-1}$ simulation, a flow with a return period lower than two years), a "pools and riffles" structure develops from the flow depth results. However, as peak flow increases (i.e., 24 $m^3 s^{-1}$ simulation, Q_2) and pools become increasingly connected to one another, this pattern fades. Finally, owing to the presence of obstacles in the form of great-sized boulders, the flow pattern (i.e., 72 $m^3 s^{-1}$ simulation) progresses toward a clearly defined main channel with high sinuosity.

Changes in water flow across the Manzanares reach and changes in flow regime are closely related. Hydraulic falls and jumps that locally modify the flow depth are associated with the topographic irregularity (stepped longitudinal profile of the river reach), which produces shifts in a flow regime from subcritical to supercritical. Furthermore, because of the limited topographic irregularity (in height, with 11 m lowering in the studied river reach), it is possible that the effect of hydraulic falls and jumps could be more evident with lower peak flows. The effect of these hydraulic falls and jumps should decrease under higher peak flows due to a generally deeper water flow where channel bottom irregularities tend to decrease.

The reduction in flow depth observed for some potholes has been facilitated by the spatial variation in the placement of hydraulic falls and jumps. In general, the flow depth at potholes location increases along with the peak flow value. This is the general trend for 28 of the 33 analyzed potholes in the Manzanares site. The 28 potholes, which show a positive correlation between peak flow and flow depth exhibit the expected pattern of behavior between both variables. However, in some groups of lateral potholes, we noted a lowering in flow depth during higher flows (54 and 72 $m^3 s^{-1}$). This effect of flow depth being lowered may be controlled by the presence of two hydraulic jumps between potholes. There are other cases where some variability across the modeled peak flows is observed. In this case, the results of the hydrodynamic models at higher modeling discharges show divergences in flow due to a "secondary channel" just upstream of the location of potholes (Fig. 13, see potholes in Fig. 2C), which may control and reduce the flow locally.

3.3.1. Spatial distribution of FFD and pothole geometry

Our findings show that potholes may follow an aggregated spatial pattern and will be separated according to their typologies (Fig. 14).

Cylindrical potholes would be expected to form in the channel center, which experiences the most flow over prolonged durations. Most of the cylindrical potholes correlate well with Q_2 discharge. The trend line shows an R^2 of 0.9. This line is slightly different, parallel, and higher than line 1:1 (equal formative and Q_2 discharge flow depths).

Compound potholes are located in the upper portion of the diagram with high values of FFD during Q_2. The old stage in evolution is represented by these potholes. Their distribution along the channel planform suggests that larger potholes will exist in local regions of the channel with strong local vorticity and high velocities and associated, greater bedload transfer (larger supply of grinders). Evidently, their present dimensions are not related to FFD. These morphotypes could also date back to a less-incised stage wherein the strath terrace was the current bed with cylindrical potholes; hence, the convolution may have occurred with these floods occurring afterwards.

Lateral potholes are primarily located in the lower part of the diagram. Thus, the theoretical formative flow is lower according to the pothole diameter, but due to their characteristics (by having breached walls), such potholes lack the ability to generate vorticity and their dimensions (diameter, depth, circularity) remain stable.

Most of the incipient potholes are located at lower values of formative flows (lower diameter) and are unable to be reached by Q_2 flow despite its low diameter because these potholes are formed on a higher bedrock bench. These potholes are unable to trap sediment owing to their limited vertical dimensions.

3.3.2. Controls of potholes growth: shear stress and sediment entrainment

Shear stress is another significant component that could control the development of potholes. We calculated the distribution of τ along the modeled section (Fig. 12) in the hydrodynamic model with the position

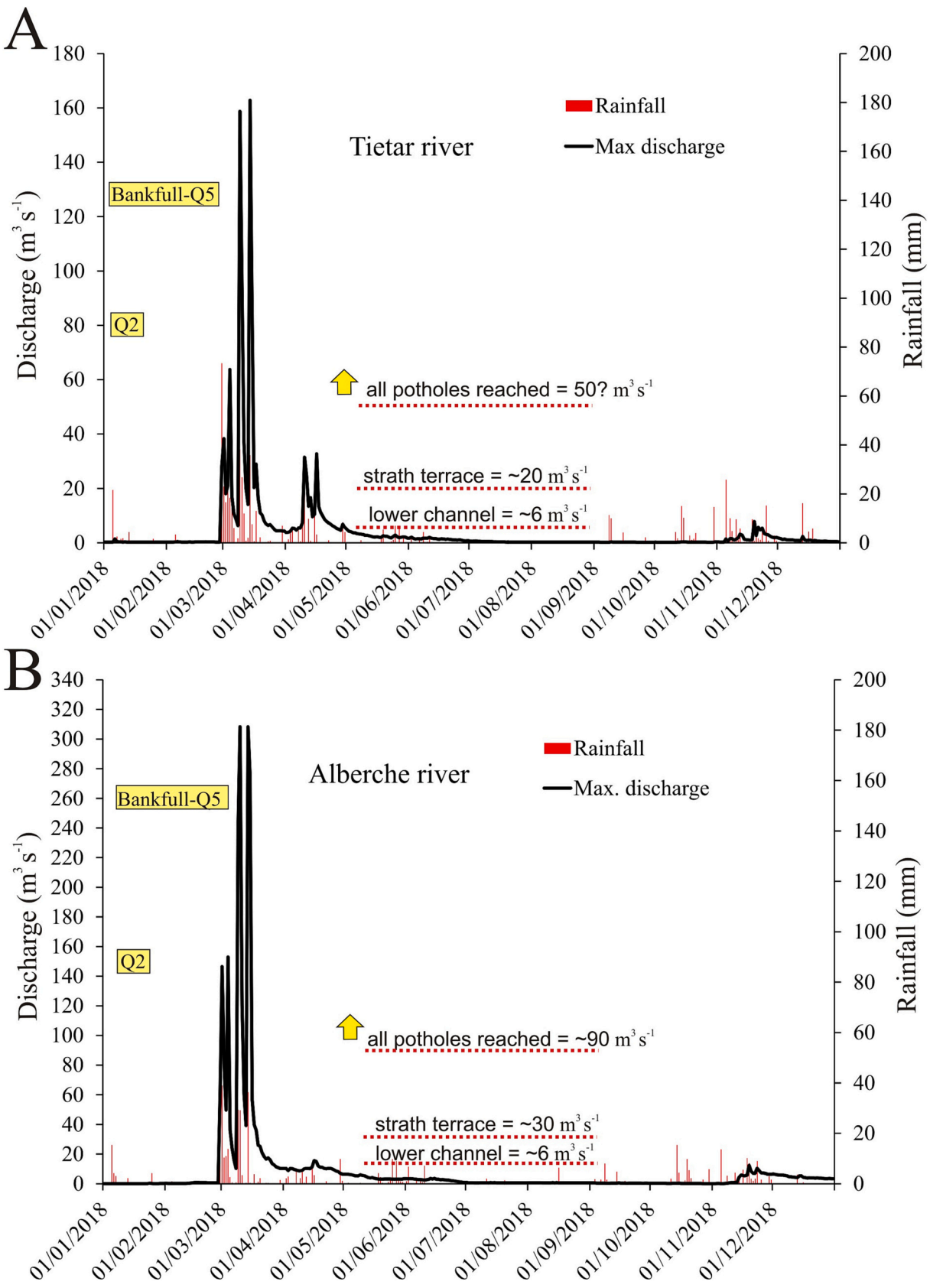

Fig. 7. Hydrograph with the discharge during the 2018 flood event affecting various pothole levels at Tietar (A) and Alberche (B) sites.

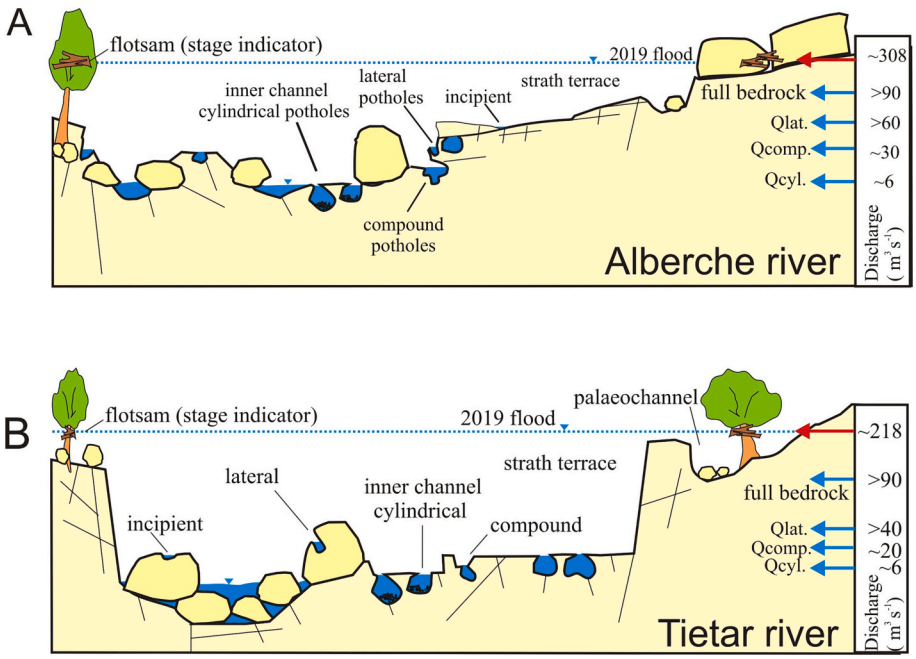

Fig. 8. Schematic picture with representation of all morphotypes and discharges affecting flow depths during the 2019 event at the Alberche (A) and Tietar (B) sites. Red arrows indicate the peak discharge in 2019; blue arrows indicate the discharge at lateral, compound, and cylindrical potholes.

of potholes (red dots and pothole number) and for all scenarios (peak flow values) considered. The results show how potholes are located in low-shear stress areas but near high shear stress values (often upstream); we should note that points in Fig. 12 simply depict the location of potholes but not their entire dimensions. The findings highlight that some potholes are linked to high shear stress values, assuming the dimensions of the pothole. The incipient and cylindrical potholes exhibit a higher mean value of shear stress from hydrodynamic results at bankfull stage (37 $m^3 s^{-1}$). For this peak flow value, the mean shear stress of incipient potholes goes up to 700 N m^{-1}, while cylindrical potholes show an average value of 650 N m^{-1}. The mean values for erosional and lateral potholes are slightly over 600 N m^{-1}, and 580 N m^{-1}, respectively. These results indicate the efficiency of the bankfull peak flow over the potholes that are still in the "construction phase", where the mean shear stress values are greater than those values for erosional and lateral potholes (both at the "destructive phase"). Furthermore, the shear stress values related to more frequent discharges (as the Q_2 and bankfull discharge, which is about Q_5) are not usually greater than those related to less frequent discharges, but combining the discharge frequency and magnitude of shear stress, we can see that more frequent flow rates are more efficient in pothole development.

Both the assumptions of D_{50} grain size (available as Table in supplementary material) and the pothole radius size as a major determinant for the settlement velocity of sediment were used to test the efficacy of sediment entrainment. Although we must take into account that nine of the 33 potholes did not contain sediment, there are some parallels and variations between the results of the two studies; therefore, one of the analyses (when using D_{50} as particle grain size) shows no results for these potholes. The findings show differences depending on the type of pothole (incipient, cylindrical, compound, or lateral).

The results highlight that lower flow rates (up to bankfull stage) are more efficient for potholes in the constructive phase (incipient and cylindrical potholes) when W_s uses pothole radius as the particle grain size (Fig. 15A). Therefore, all (3) incipient potholes show a Rouse number lower than 7.5 for bankfull stage flow, as do half of the cylindrical potholes (the other ones require a flow rate higher than $Q_{25} = 72\ m^3 s^{-1}$, suggesting their being in a degradational phase). Frequent flow rates (the ones with a return period lower than 25 years) show less efficacy for compound and lateral potholes, which may be related to a destructive phase. Compound and lateral potholes account for 24 of the 33 potholes present at the Manzanares study site, and 15 of these 24 potholes do not show a Rouse number lower than 7.5 for flow rates with a return period of 25 years or less.

When the D_{50} grain size is used for W_s calculation, the results are slightly different (Fig. 15B), which is partially due to the absence of sediment in nine out of 33 potholes at the Manzanares study site. In any case, the effectiveness of frequent flow rates (up to Q_{25}) is significantly higher than previously noted, and 19 out of 33 potholes have effective sediment transport (for D_{50} grain size) with flow rates as low as 5 $m^3 s^{-1}$. From all potholes, only one (compound class) does not have effective sediment transport for the set of flow rates used in the present studio and needs a flow rate higher than 72 $m^3 s^{-1}$ (25-year return period peak flow) for D_{50} grain size movement. Due to geometric restrictions, the compound and lateral potholes, which are those related to a destructive phase, show most of the "sediment absent" potholes, although the rate of "sediment absent" potholes is higher in the incipient potholes where only one of the three potholes contain sediment inside.

When considering full sediment entrainment (i.e., the Rouse number is much lower than 7.5 for sediment grain size, similar to pothole radius), which describes the scenario where potential pothole growth rate is higher (according to Julien, 1998), the 2-year return period flow rate appears to be the one producing the optimal results for incipient and cylindrical potholes. To prevent lateral and compound potholes, a higher flow rate is required. Most compound potholes must have a flow rate higher than a 25-year return period flow rate; lateral potholes show a mixed pattern, with some exhibiting full sediment entrainment with lower flow rates and others showing characteristics similar in nature to compound potholes.

4. Discussion

The results support the hypothesis that (1) there are differences in pothole typologies distribution along the three studied sites (Fig. 3), from the studied potholes; (2) cylindrical ones are the best indicator for current discharge conditions and enable an understanding of their formative processes; (3) the proportion of other erosional features may

Fig. 9. Pictures of flood events at 21, 7.5, and 0.5 $m^3 s^{-1}$ at the Tietar site (A, upstream at rapids, B, inner channel). C. Strath terrace and potholed inner channel with interpreted flow depths at 20 (yellow, inner channel), 40 (blue, strath terrace and lateral potholes), and ~200 $m^3 s^{-1}$ (2019 peak flow, white).

tell us the degree of senescence of certain parts of the channel in a river reach or the change in its discharge conditions; and (4) we must further examine the role of Q_2 and bankfull discharge as a sculpted mechanism via abrasion and the potential of low-magnitude flows for maximizing formative conditions, however, larger discharges and other processes may still have an unknown imprint that should be carefully studied.

4.1. The spatial distribution of pothole typologies in bedrock channel

We addressed the question of what sets the spatial distribution and location of potholes in river channels. The seemingly "chaotic distribution" reflects the response of the reach to factors such as discharge, lithology, fractures, and degree of weathering. Specifically, we draw attention to the concentration of cylindrical potholes along knickpoints, which are the most effective areas in terms of pothole growth. According to Ji and Li (2019) findings, the large rock along the knickpoint in the Manzanares reach favors their cylindrical feature; however, we also find other potholes in Alberche that maintain cylindrical shape with small depth dimensions in comparison with their diameter but with signals of plucking and out of KP areas.

We interpreted the compound features to be the remains of previous potholes. The abundance of those morphotype may suggest the relict character (as Sato and Hayami, 1987 suggests) of the entire or specific portions of a bedrock reach. These findings are in consonance of those of Kale and Shingade (1987), who found that compound potholes tended to be concentrated along the channel center. Lateral potholes reflect KP upstream migration and channel formation through the width adjustments suggested by Finnegan et al. (2007). Moreover, we observed two groups of lateral potholes: those whose FFD is reached at ~ Q_2 and another group > Q_{25}. These findings could indicate that the first group is closely related to the present upstream migration of the knickpoint (as we noted in the Alberche and Manzanares rivers) and, therefore, more connected to present flow conditions, while the second group is disconnected from the present river dynamics and maybe related to an

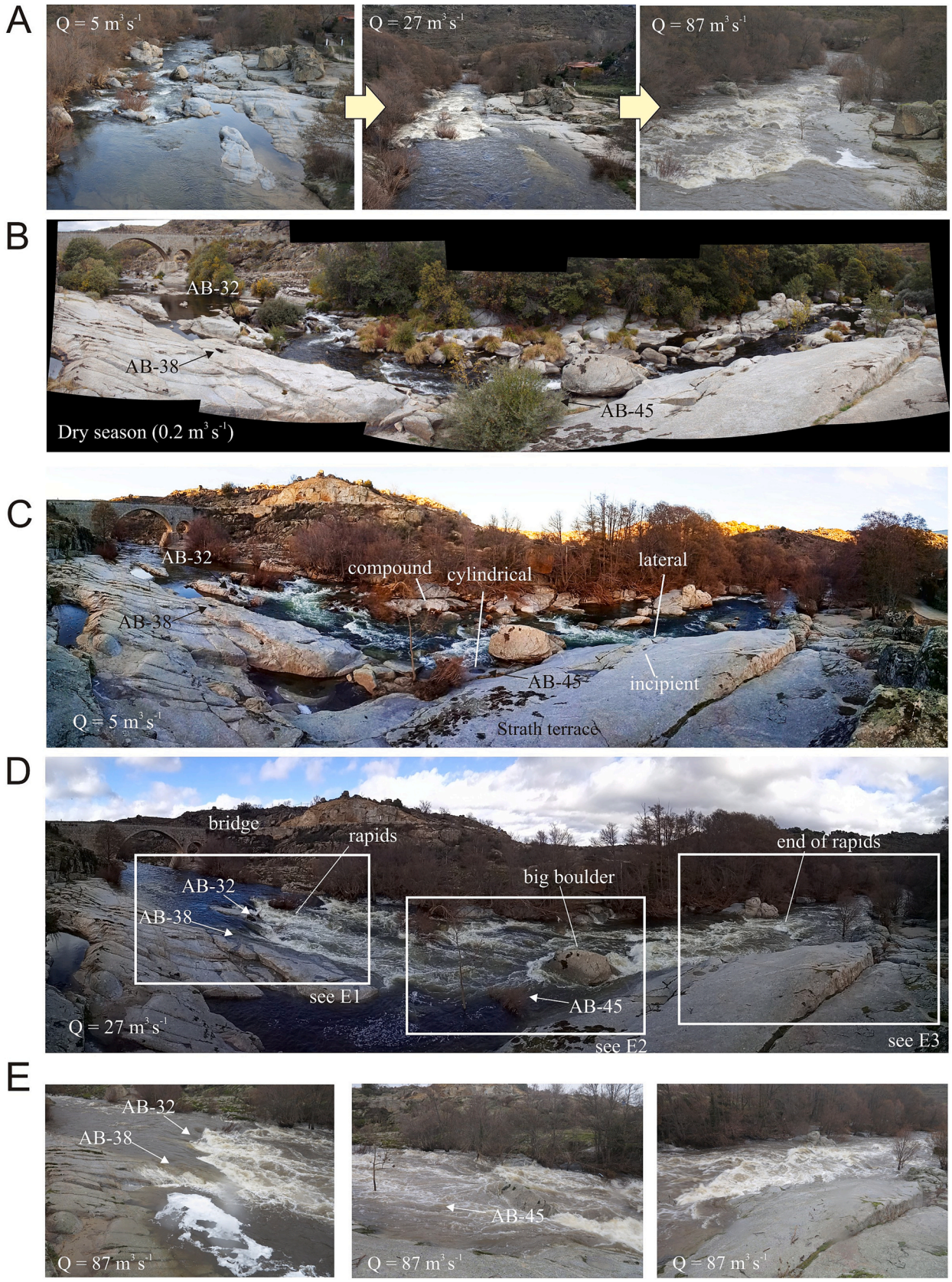

Fig. 10. Pictures taken at several flow-stage discharges at 0.2, 5, 27, and 87 $m^3 s^{-1}$ at the Alberche site. A. View from upstream to downstream at various stages, B. Dry season view with some characteristics potholes, C. Low discharge stage at 5 $m^3 s^{-1}$, D. View of ~30 $m^3 s^{-1}$ with the water depth at rapid and strath terrace, E. Flood level at 87 $m^3 s^{-1}$ reaching the top of lateral potholes and covering the rest.

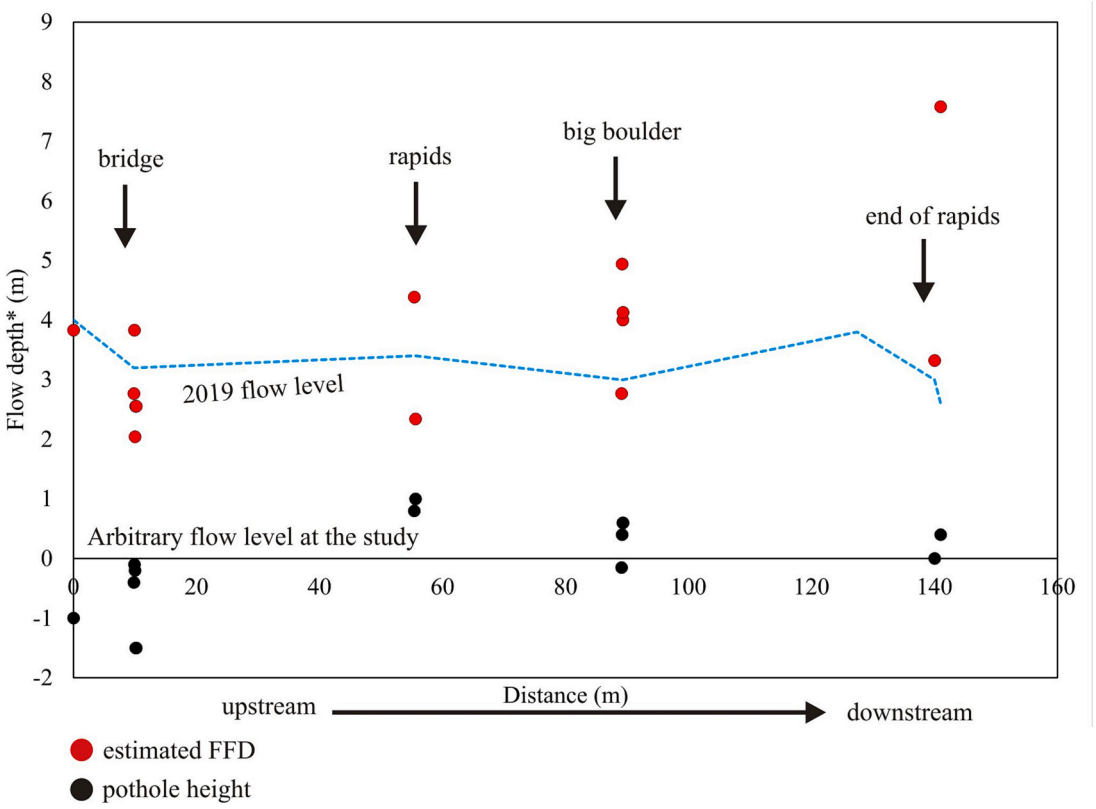

Fig. 11. Estimated FFD (red dots) above cylindrical pothole height (black dots) and maximum water flow depth at the 2019 event (blue dashed line) at the Alberche site (see Fig. 10D).

older stage (i.e.; strath terrace).

Some of the spatial patterns have other important factors not considered in detail in this study, such as i) lithology, which controls pothole dimensions (Ji and Li, 2019), ii) weathering (in the area has also been reported previously by Ortega-Becerril et al. (2017) as the inhibition of incipient potholes with the existence of well-developed planar structures parallel to the surface, which lead to weathering processes) and iii) the role of fractures in pothole development along well-jointed rock that is easy to remove, although other authors (Elston, 1917; Springer et al., 2006; Ortega et al., 2014) found a strong correlation between fractures and potholes. We observed that potholes correlate more strongly with fracture orientation and substrate resistance than with hydraulics when we consider the whole pothole population (Ortega et al., 2014; Ortega-Becerril et al., 2017).

The results from the present research indicate a strong correlation between hydraulics and cylindrical potholes but a low correlation with other pothole typologies (Fig. 14). The FFD results using the 2D hydrodynamic model in cylindrical potholes suit the bankfull discharge in five of the six studied potholes in Manzanares river. We discovered a single cylindrical pothole outlier (pothole MCV-61, former KP) far downstream from the present knickpoint that did not correlate well with Q_2 discharge, perhaps indicating the importance of active knickpoint on pothole shape. The importance of the position of active potholes under the current flow conditions is reinforced by these findings.

4.2. Formative flows

In this section, we discuss the role of low-magnitude floods (Q_2 and bankfull-Q_5) as sculpting mechanisms via abrasion. The "formative flows" where pothole depth is most significantly connected with shear stress at low flows, as opposed to "destructive flows," where medium- and high-magnitude floods with high geomorphic change (Costa and O'Connor, 1995; Wohl, 2000) were the dominant mode of bedrock removal (Dubinski and Wohl, 2013).

Pothole geometry is known to be a good indicator of hydraulic conditions. The aspect ratio serves as a dimensional threshold for the successful growth of potholes (Pelletier et al., 2015; Ji and Li, 2019). We obtained these thresholds (FFD) in every studied reach while considering all potholes, regardless of their typology. The results indicate that the Manzanares and Alberche rivers have better constrained data than Tietar (Fig. 5), which suggests the relict nature of this reach. Compared to the study of the entire population of potholes, cylindrical potholes produce better FFD results with less dispersion (Fig. 6). However, we observed changes in results due to variations of bedrock lithology, as seen in Manzanares with microdiorite dikes. The width of dikes (up to ~50 cm) constrained and limit the expansion of potholes.

Since FFD acts as a theoretical threshold, we also analyze the importance of the effective growth geometry with real discharge in gauged and ungauged sites. The full coverage of all potholes at the two gauged sites (Alberche and Tietar) is less than the value of Q_2 and bankfull depth, therefore demonstrating the high frequency of effective working.

To determine whether FFD was reached in cylindrical potholes, we utilize the high water marks (HWM) from the 2019 flood in the Alberche river, which are slightly higher than bankfull depth (Fig. 11). The results indicate that only a group of potholes fall below the threshold. However, a detailed analysis of potholes reveals that not all cylindrical potholes recorded can be considered "active potholes." In this analysis, truncated potholes and quasi-cylindrical were avoided.

We used the ungauged basin of Manzanares to test the 2D hydrodynamic model and the theoretical threshold of FFD provided by pothole geometry. We deep into a knowledge gap; the genesis and formative processes of bedrock features, poorly understood in bedrock channel geomorphology (Lamb et al., 2015). Using current knickpoint cylindrical potholes, we discovered good correlations of $R^2 = 0.91$ between FFD and Q_2 flow (Fig. 14). However, the compound and lateral

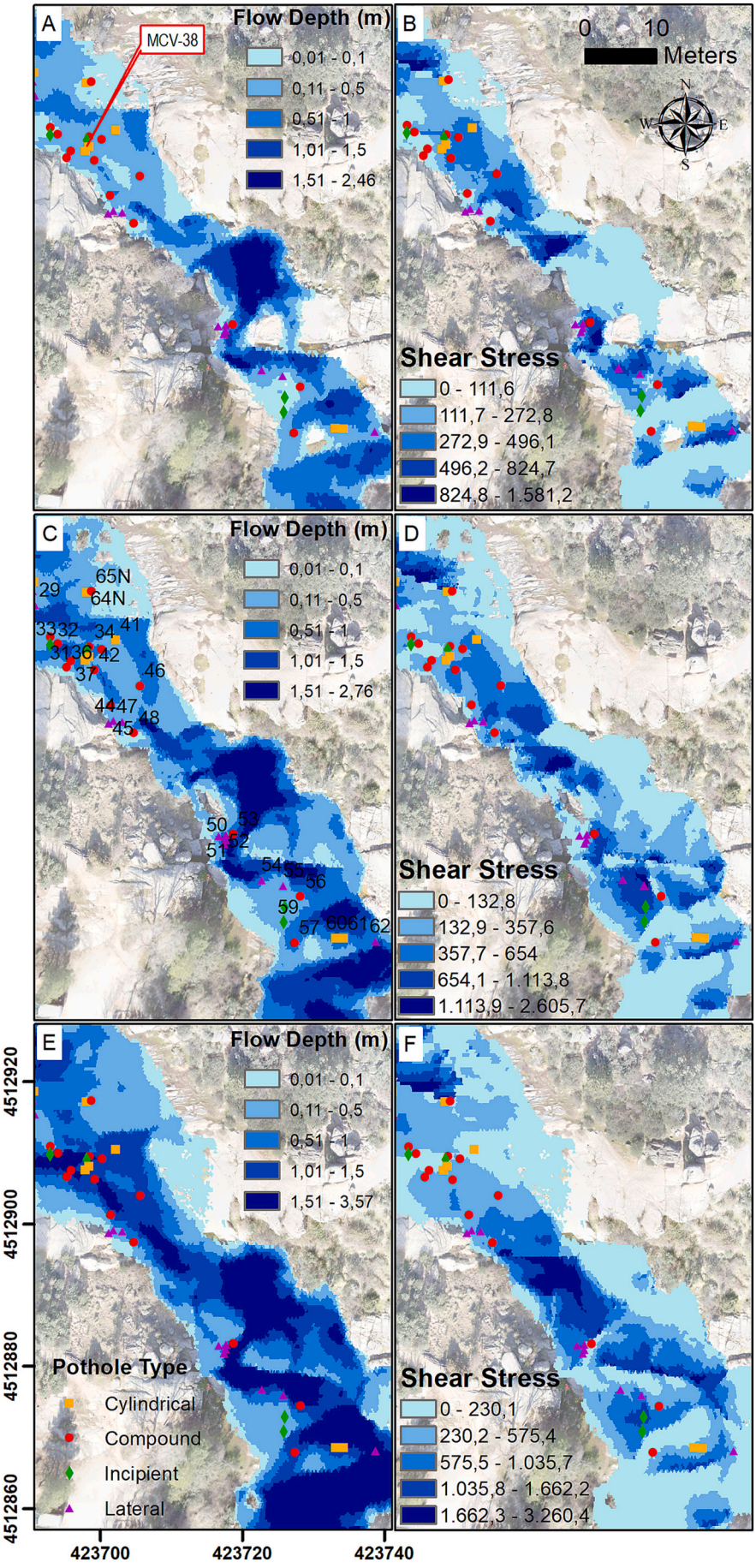

Fig. 12. Hydrodynamic model results for Manzanares R. Water flow changes (from water depth results: A: 10 m^3 s^{-1}, C: 24 m^3 s^{-1}, E: 72 m^3 s^{-1}) are related to rising peak flow values. For higher peak flow, water conveys, forming a clear main channel, while a rhythmic "pool-rapid" succession is observed in lower peak flow. The pothole MCV-38 shows location of KP. The right column shows shear stress values for 10 m^3 s^{-1} (B); Q_2, 24 m^3 s^{-1} (D); and Q_{25}, 72 m^3 s^{-1} (F). In all figures, the flows are in the south-east direction.

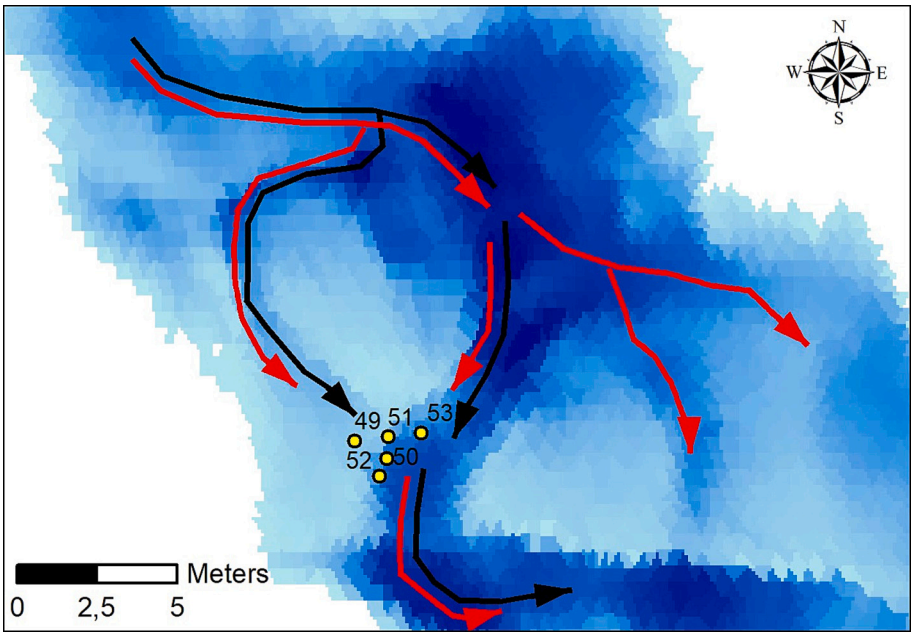

Fig. 13. Flow path changes related to increasing peak flow value from 54 to 72 $m^3 s^{-1}$. Black arrows show the main flow paths for 54 $m^3 s^{-1}$, while red arrows show the flow paths for 72 $m^3 s^{-1}$.

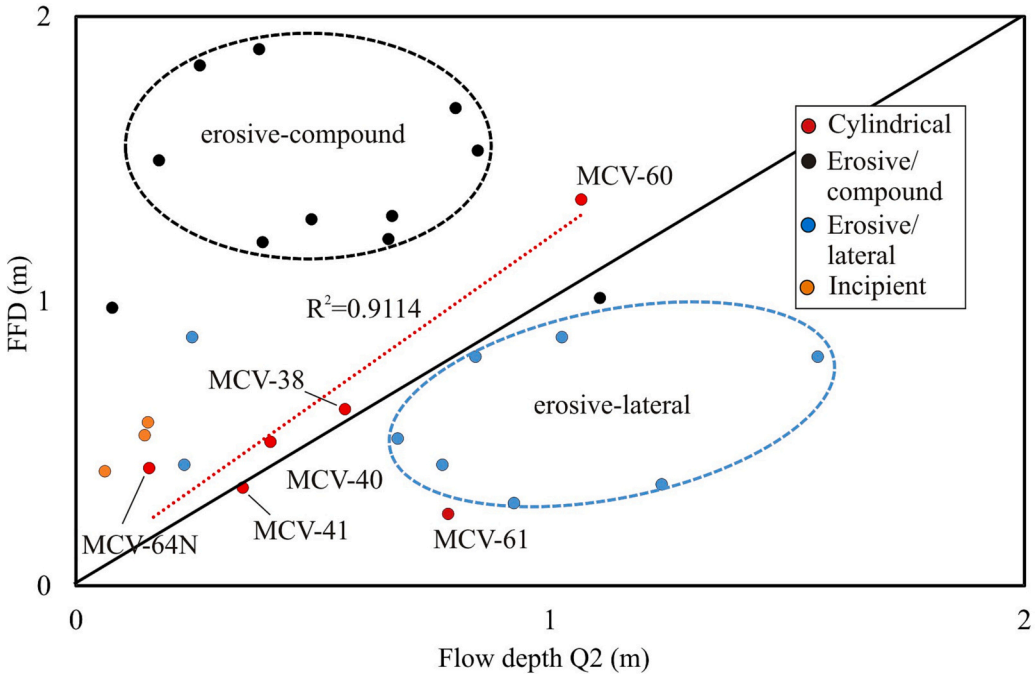

Fig. 14. Formative flow depth of Manzanares potholes vs. modeled flow depth at Q_2 discharge (24 $m^3 s^{-1}$). Black circle shows the most compound potholes; blue circle shows the distribution of lateral potholes; red line shows the trend line adjustment of cylindrical potholes at the present knickpoint.

potholes indicate FFDs that do not fit well with the 2D model. Therefore, we consider these features poor indicators of the degree of activity of flow, and their growth and current evolution are likely more closely related to erosive episodes of medium-high flood magnitude as they are remnant features and are not driven by FFD. Our findings confirm Zen and Prestegaard's (1994) theory that pothole formation occurs significantly near bankfull flows and also confirms Thompson (1990) statement that "features are genetically related to frequent, intensely erosive flood discharges".

The results indicate that FFD appears to be strongly influenced by channel gradient and that differences in channel gradient between river reach scale and local (or pothole scale) may alter the FFD results. At the Manzanares study site, the channel gradient seems higher than the river reach scale gradient, although the results show more variability and are likely more susceptible to DEM errors and limitations (related to the ability to represent large gradient of the terrain). Thus, all potholes (including compound ones) reached the FFD lower limit for the river bankfull stage (37 $m^3 s^{-1}$) when local (pothole) scale channel gradient was employed to obtain FFD values. For most of incipient potholes, cylindrical potholes, and lateral potholes, the lower boundary of FFD was reached with a flow rate as low as 5 $m^3 s^{-1}$ (the lowest in our analysis).

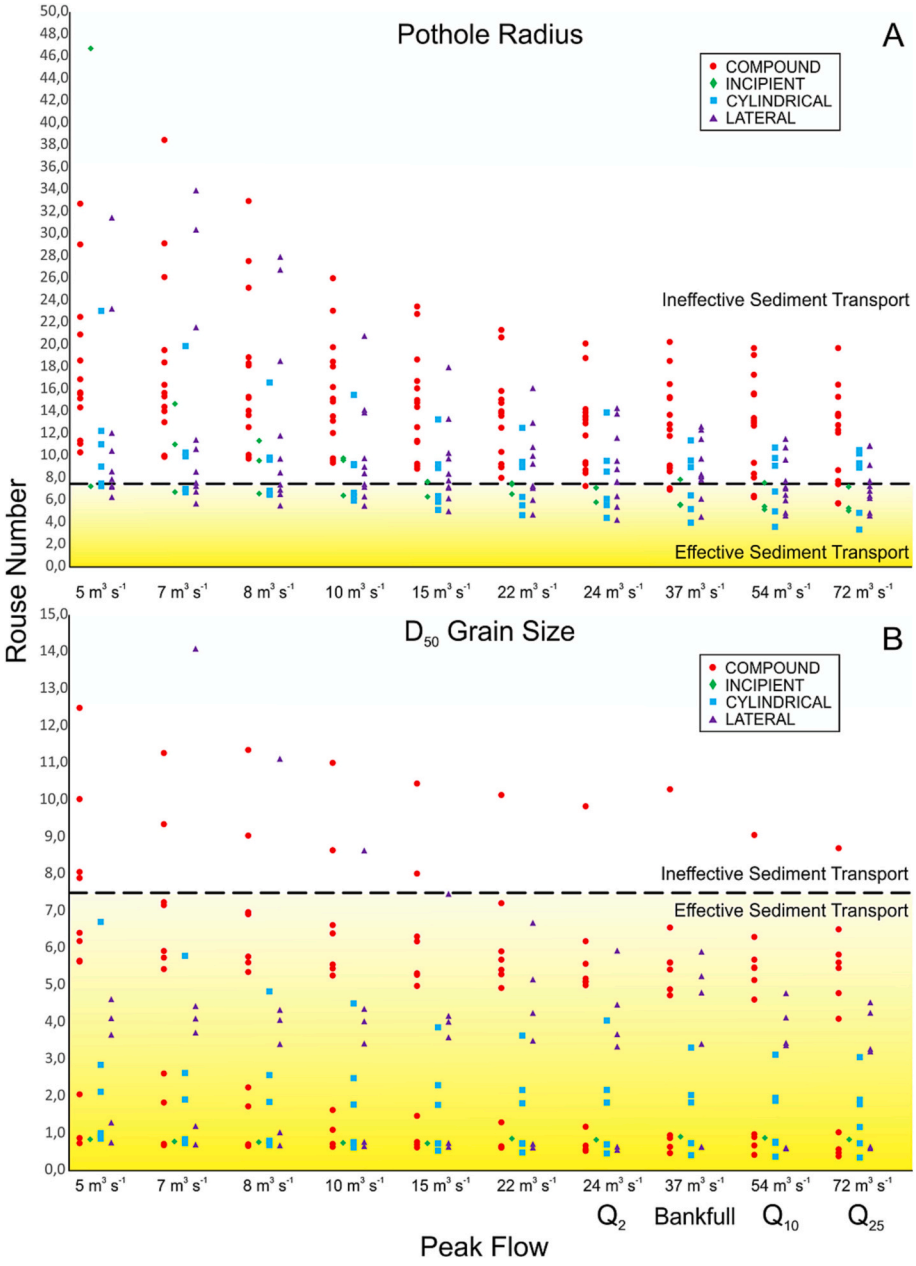

Fig. 15. A. Rouse number results for potholes at the Manzanares study site using D_{50} grain size in sediment settling velocity estimation. B. Rouse number results for potholes at the Manzanares study site using the pothole radius in sediment settling velocity estimation. Based on the Rouse number limit of 7.5, sediment movement is classified as effective and ineffective. Note A and B shows different Y-axis ranges to optimize data visualization.

We also must consider that the flow depth (or the FFD value) is not necessarily the only parameter for pothole development; variables such as lithology, fractures, changes in mineral concentrations, weathering, etc., have been outlined by other authors (e.g., Kale and Shingade, 1987; Yin et al., 2016; Ji and Li, 2019; Jantzi et al., 2020; Bera et al., 2021) to play a key role too.

4.3. Flow shear stress and sediment entrainment

Using sediment entrainment and shear stress, we assess the response of different pothole typologies to various discharges through the use of the Rouse number. The FFD and Rouse number results do not always point out in the same direction, and the Rouse number typically narrows the flow rates range at which effective sediment entrainment occurs.

The results obtained for the Rouse number in the vicinity of potholes seem to be dependent on sediment size as this parameter affects the settling velocity. When the Rouse number is lower than 7.5 for sediment size equal to the potholes radius, the sediment entrainment rate, which is connected to the constructive or destructive rates of potholes, is at its highest.

The results of compound and lateral potholes (to a lesser extent) demonstrate that flow rates up to 25-year return period peak flows are ineffective for the majority of potholes in the "destructive phase". Higher flow rates (particularly when pothole radius defines the grain size in settling velocity estimation) are associated with the maximum efficiency in sediment entrainment and the evolution of potholes (both constructive and destructive works). The destructive evolution of those potholes seems to be related to higher flow rates and not to FFD.

For potholes that are still in constructive phase, high frequency flow rates (such as bankfull flow rate, or the 10-year return period peak flows) can entrain sediment from potholes and thereby lead to their constructive development, even when using pothole radius as grain size

in the calculation of settling velocity. This is theoretically possible for the both incipient and cylindrical types, although these groups of potholes are unable to store sediment grains due to their open morphology. The latter show greater variability. A few cylindrical pothole sizes and, thus, pothole radius used in settling velocity show dimensions that are incompatible with effective sediment entrainment for low and more frequent flow rates, hence requiring flow rates related to flood events above a 25-year return period, which may be reflected in the results obtained (Fig. 15A). This group appears to be closer to reaching its development limit and transitioning to a destructive phase.

However, this does not rule out effective sediment entrainment (and constructive or destructive developments of potholes) for lower flow rates as this will be able to move finer sediment particles, which can produce pothole evolution as Yin et al. (2016) noted, and thus promote pothole evolution at lower rates or velocities. The occurrence of effective sediment entrainment for finer particles (up to D_{50} grain sizes) initiates low flow rates, according to our results at the Manzanares study site, which permits the development of incipient potholes over a long period of time. All potholes in the constructive phase (incipient and cylindrical potholes) suffer "theoretical" sediment entrainment for flow rates as low as 5 $m^3\ s^{-1}$, which indicates that pothole development occurs almost constantly albeit at small rates. Moreover, this trend works and is accelerated for higher flow rates.

All those results have some uncertainty due to the use of a 2D hydrodynamic model instead of a 3D model. The 2D models average the results of output variables on the *Z*-axis. So, the shear stress at the base of the pothole could be lower than at the inner channel bed. The authors assume this limitation, and the simplification it implies in the hydrodynamic model. However, the authors consider the 2D model approach to the analysis valid due to several factors: i) the use of a high resolution DEM that can approximate the shape of the potholes, especially the larger ones; ii) the use of average values of the output variables (as flow depth or shear stress) in the immediate surroundings of the pothole can approximate the areas with the most favorable conditions for the onset of erosion and the existence of favorable conditions for the pothole development; and iii) the present work focuses on the conditions that promote the initiation of constructive development of potholes, where the initial phase of these forms are reproduced by the DEM.

4.4. Future work

This study serves as the foundation for more in-depth research and 2D models. We plan to apply 2D hydraulic modeling to all sites. This would enable us to understand how well potholes currently function. It would be interesting to learn about the "**cover effect**" of sediments (Turowski et al., 2007; Nelson and Seminara, 2011; Beer et al., 2017) in these channel sections and the high-depth "**protection layer**" of bedrock bounds during major floods. This may disable macroturbulence and the formation of a stationary vortex. Furthermore, we found some potholes that were filled with sediments; these features were unable to exceed shear stress and became ineffective unless a major flood occurred. Perhaps this is somehow related to grain size (e.g., a 30-cm median grain size needs a settling velocity of ~1.8 m/s and would require shear stresses on the order of ~3000 Pa, far higher than the values we obtained in the hydrodynamic model). Grain size plays a key role in the sediment entrainment process because it limits the range of peak flow for effective transport and pothole development. The sediment trapped in the potholes clearly shows two behaviors: i) the potholes located above the knickpoint are mostly clean or with some very fine-sized sediment, while ii) the potholes downstream of the knickpoint contain more sediment and are larger in size. Flow divergence is observed in some cases, with more energetic clean zones, such as those shown in Fig. 13, whereas there are low velocity/sedimentation zones with larger boulders, coincident with large compound potholes in destructive phase. However, the effectiveness of sediment entrainment at lower peak flows necessitates further attention as it is possible that the river flow cannot entrain all the sediment from the pothole but can move the finer sediment, which can cause the pothole to evolve at a lower rate. Moreover, another key point, as previously noted by Wohl and Ikeda (1997), is the role of shallow flow depths, which requires in-depth investigation.

5. Conclusion

The purpose of this research was to investigate whether different pothole typologies are located and distributed along any specific areas related to certain discharges (formative flows) and flow depths (FFD). Our main conclusions are as follows.

- The frequent Q_2 and bankfull depths completely cover all pothole typologies along the three studied sites. These depths can be considered the current FFD in active potholes.
- This situation is insufficient to reach their FFD in the more evolved and erosive pothole typologies. This would mean i) those erosive potholes need higher discharges to attain an effective flow depth or ii) the erosive features are being generated by catastrophic events that produce their breakup rather than by constant abrasion.
- The comprehensive 2D hydrodynamic model in Manzanares river shows that cylindrical pothole dimensions are closely related to bankfull discharge, which is considered the effective FFD. It appears that compound and lateral potholes are remnants of older conditions. Younger laterals potholes, linked to knickpoint evolution, demonstrate FFD near bankfull flows.
- The position of potholes does not follow a random pattern according to its typology. The development of potholes along the channel and their shift from active to senile state are caused by current and historical flow conditions. Sediment entrained in potholes suggest a key role of knickpoint with clean areas upstream KP and sediment filled potholes downstream. Also flow divergence in a section under certain discharges may separate active from senile potholes.
- Our research may serve as a starting point for future studies related to understand the fluvial processes (macro and microabrasion, plucking, etc.) linked to sculpted forms morphology.

Supplementary data to this article can be found online at https://doi.org/10.1016/j.geomorph.2023.108738.

Declaration of competing interest

The authors declare that they have no known competing financial interests or personal relationships that could have appeared to influence the work reported in this paper.

Data availability

No data was used for the research described in the article.

Acknowledgments

We thank Geohazards InSAR laboratory and Modelling Group (IGME-CSIC) for assistance on airborne scan used on DEM models. The authors thank Michael Lamb for field discussions. We also give thanks to Ellen Wohl and Joel Scheingross for stimulating discussions that helped develop this manuscript. This work was supported by Top Heritage (P2018/NMT-4372) program from the Regional Government of Madrid (Spain).

References

Alexander, H.S., 1932. Pothole erosion. J. Geol. 40 (4), 305–337. https://doi.org/10.1086/623954.

Álvarez-Vázquez, M.Á., De Uña-Álvarez, E., 2017. Growth of sculpted forms in bedrock channels (Miño River, northwest Spain). Curr. Sci. 112 (5), 996–1002. http://www.jstor.org/stable/24912491.
Arcement, G.J., Schneider, V.R., 1989. Guide for selecting Manning's roughness coefficients for natural channels and flood plains. In: Water Supply Paper 2339. USGS, Denver.
Baker, V., 1973. Paleohydrology and sedimentology of Lake Missoula flooding in eastern Washington, 79p. Geol. Soc. Am. Spec. 144, 1973.
Baker, V.R., Kale, V.S., 1998. The role of extreme floods in shaping bedrock channels. Geophysical Monograph-American Geophysical Union 107, 153–166.
Beer, A.R., Turowski, J.M., Kirchner, J.W., 2017. Spatial patterns of erosion in a bedrock gorge. J. Geophys. Res. Earth Surf. 122 (1), 191–214. https://doi.org/10.1002/2016JF003850.
Bera, B., Bhattacharjee, S., Ghosh, A., Ghosh, S., Chamling, M., 2019. Dynamic of channel potholes on Precambrian geological sites of Chhota Nagpur plateau, Indian peninsula: applying fluvio-hydrological and geospatial techniques. SN Appl. Sci. 1 (5), 1–14. https://doi.org/10.1007/s42452-019-0516-2.
Bera, B., Bhattacharjee, S., Chamling, M., Ghosh, A., Sengutpa, N., Ghosh, S., 2021. Relationship between diameter and depth of potholes controlled by lithology and structure in the Rarh region of India. Curr. Sci. 121 (5), 697–703.
Bladé, E., Cea, L., Corestein, G., Escolano, E., Puertas, J., Vázquez-Cendón, E., Dolz, J., Coll, A., 2014 (in spanish). Iber: herramienta de simulación numérica del flujo en ríos. Rev. Int. Metodos Numer. para Calc. Diseno Ing. 30(1), 1–10.
Charpentier, J.F., 1841. Essai sur les glaciers: Et sur le terrain erratique du bassin du Rhône. Lausanne, M. Ducloux, p. 363.
Chow, V.T., 1959. Open-Channel Hydraulics. The Blackburn Press, West Caldwell, United States.
Costa, J.E., O'Connor, J.E., 1995. Geomorphically effective floods. Natural and anthropogenic influences in fluvial geomorphology. Geophys. Monogr. Ser. AGU 89, 45–56.
Das, B.C., 2018. Development of streambed potholes and the role of grinding stones. J. Environ. Geogr. 11 (1–2), 9–16. https://doi.org/10.2478/jengeo-2018-0002.
Dubinski, I.M., Wohl, E., 2013. Relationships between block quarrying, bed shear stress, and stream power: a physical model of block quarrying of a jointed bedrock channel. Geomorphology 180-181, 66–81. https://doi.org/10.1016/j.geomorph.2012.09.007.
Elston, E.D., 1917. Potholes: their variety, origin and significance (I). Sci. Mon. 5, 554–567.
Ferguson, R.I., Church, M., 2004. A simple universal equation for grain settling velocity. J. Sediment. Res. 74 (6), 933–937. https://doi.org/10.1306/051204740933.
Finnegan, N.J., Sklar, L.S., Fuller, T.K., 2007. Interplay of sediment supply, river incision, and channel morphology revealed by the transient evolution of an experimental bedrock channel. J. Geophys. Res. Earth Surf. 112 (F3) https://doi.org/10.1029/2006JF000569.
Gomez-Heras, M., Ortega-Becerril, J.A., Garrote, J., Fort, R., Lopez-Gonzalez, L., 2019. Morphometric measurements of bedrock rivers at different spatial scales and applications to geomorphological heritage research. Prog. Earth Planet. Sci. 6 (1), 29. https://doi.org/10.1186/s40645-019-0275-0.
Goode, J.R., Wohl, E.E., 2010. Substrate controls on the longitudinal profile of bedrock channels: implications for reach-scale roughness. J. Geophys. Res. Earth Surf. 115, F03018. https://doi.org/10.1029/2008JF001188.
Heitmuller, F.T., Hudson, P.F., Asquith, W.H., 2015. Lithologic and hydrologic controls of mixed alluvial–bedrock channels in flood-prone fluvial systems: Bankfull and macrochannels in the Llano River watershed, central Texas, USA. Geomorphology 232, 1–19. https://doi.org/10.1016/j.geomorph.2014.12.033.
Jantzi, H., Carozza, J.M., Probst, J.L., 2020. Sculpted forms into bedrock channel: typology, spatial distribution and implications for channel dynamic. Insight from molassic knickpoints on the Middle Garonne (South-West France). Geomorphol. Relief, Process. Environ. 26 (2).
Jennings, J.N., 1983. Swirlholes and related bedrock river channel forms. Aust. Geogr. 15 (6), 411–414. https://doi.org/10.1080/00049188308702846.
Ji, S., Li, L., 2019. Characterization of Stream Potholes in Interlayered Felsic and Mafic Gneisses from the Deerfield River, Shelburne Falls (Massachusetts, USA), and Implications for River Incision into Bedrock. J. Geol. 127 (2), 183–205. https://doi.org/10.1086/701517.
Ji, S., Li, L., Zeng, W., 2018. The relationship between diameter and depth of potholes eroded by running water. J. Rock Mech. Geotech. Eng. 10 (5), 818–831. https://doi.org/10.1016/j.jrmge.2018.05.002.
Ji, S., Zeng, W., Li, L., Ma, Q., Feng, J., 2019. Geometrical characterization of stream potholes in sandstone from the Sunxi River (Chongqing, China) and implications for the development of bedrock channels. J. Asian Earth Sci. 173, 374–385. https://doi.org/10.1016/j.jseaes.2019.01.037.
Jiménez Álvarez, A., García Montañes, C., Mediero Orduña, L., Incio Caballero, L., Garrote Revilla, J., 2013. Bases metodológicas del mapa de caudales máximos de las cuencas intercomunitarias. Servicio Publicaciones CEDEX, Madrid, España, p. 97 (in spanish).
Johnson, J.P., Whipple, K.X., 2007. Feedbacks between erosion and sediment transport in experimental bedrock channels. Earth Surf. Process. Landf. 32 (7), 1048–1062. https://doi.org/10.1002/esp.1471.
Julien, P.Y., 1998. Erosion and Sedimentation. New York, Cambridge Univ. Press, p. 280.
Kale, V. S., Shingade, B. S., 1987. A morphological study of potholes of Indrayani knickpoint (Maharashtra). V.S. Datya (Ed.), Explorations in the Tropics, Professor K. R, Dikshit Felicitation Committee, Pune, India (1987), pp. 206–214.
Kanhaiya, S., Singh, S., Singh, C.K., Srivastava, V.K., 2019. Pothole: a unique geomorphological feature from the bedrocks of Ghaghghar River, Son valley, India. Geol. Ecol. Landsc. 3 (4), 258–268.
Lamb, M.P., Finnegan, N.J., Scheingross, J.S., Sklar, L.S., 2015. New insights into the mechanics of fluvial bedrock erosion through flume experiments and theory. Geomorphology 244, 33–55. https://doi.org/10.1016/j.geomorph.2015.03.00.
Leopold, L., 1994. A View of the River. Cambridge, Massachusetts, Harvard Univ. Press, p. 320.
Lorenc, M.W., Saavedra, J., 1980. Remarks on the pothole erosion at the Tormes (Salamanca province, Spain). Acta Geol. Hisp. 15, 91–93.
Lorenc, M.W., Barco, P.M., Saavedra, J., 1994. The evolution of potholes in granite bedrock, W Spain. Catena 22 (4), 265–274. https://doi.org/10.1016/0341-8162(94)90037-X.
Mosley, M.P., 1981. Semi-determinate hydraulic geometry of river channels, South Island, New Zealand. Earth Surf. Process. Landf. 6 (2), 127–137. https://doi.org/10.1002/esp.3290060206.
Nelson, P.A., Seminara, G., 2011. Modeling the evolution of bedrock channel shape with erosion from saltating bed load. Geophys. Res. Lett. 38, L17406. https://doi.org/10.1029/2011GL048628.
Nemec, W., Lorenc, M.W., Saavedra, J., 1982. Potholed granite terrace in the rio Salor valley, western Spain : a study of bedrock erosion by floods. Tecniterrae 50, 6–21.
Ortega, J.A., Gómez-Heras, M., Perez-López, R., Wohl, E.E., 2014. Multiscale structural and lithologic controls in the development of stream potholes on granite bedrock rivers. Geomorphology 204, 588–598. https://doi.org/10.1016/j.geomorph.2013.09.005.
Ortega-Becerril, J., Gomez-Heras, M., Fort, R., Wohl, E., 2017. How does anisotropy in bedrock river granitic outcrops influence pothole genesis and development? Earth Surf. Process. Landf. 42 (6), 956–968. https://doi.org/10.1002/esp.4054.
Pelletier, J.D., Sweeney, K.E., Roering, J.J., Finnegan, N.J., 2015. Controls on the geometry of potholes in bedrock channels. Geophys. Res. Lett. 42, 797–803. https://doi.org/10.1002/2014GL062900.
Richardson, K., Carling, P.A., 2005. A typology of sculpted forms in open bedrock channels. Geol. Soc. Am. Spec 392, 1–108.
Sato, S., Hayami, T., 1987. Potholes in Shikoku, Japan: Part II. Origin of potholes and significance of pothole research. Mem.Fac.Educ., Ehime Univ., Ser.III 7, 191–220.
Sato, S., Matsuura, H., Miyazaki, M., 1987. Potholes in Shikoku, Japan: Part I. Potholes and their hydrodynamics in the Kurokawa River, Ehime. Mem. Fac. Educ., Ehime Univ., Ser. III 7, 127–190.
Sherwood, J.M., Huitger, C.A., 2005. Bankfull Characteristics of Ohio Streams and Their Relation to Peak Streamflows (No. FHWA/OH-2005/004). US Department of the Interior, US Geological Survey, Columbus.
Singtuen, V., Junjuer, T., 2022. Characterisation of potholes formed on bedrock sandstones at Loei Dun, Phetchabun Geopark, Thailand. Geologos 28 (1), 39–50. https://doi.org/10.2478/logos-2022-0003.
Springer, G.S., Tooth, S., Wohl, E.E., 2005. Dynamics of pothole growth as defined by field data and geometrical description. J. Geophys. Res. Earth Surf. 110. F04010 https://doi.org/10.1029/2005JF000321.
Springer, G., Tooth, S., Wohl, E.E., 2006. Theoretical modelling of stream potholes based upon empirical observations from the Orange River, Republic of South Africa. Geomorphology 82, 160–176. https://doi.org/10.1016/j.geomorph.2005.09.023.
Thompson, G.H., 1990. Geomorphology of the Lower Susquehanna River gorge: Lancaster, Pennsylvania, Pennsylvania Geologists 55th Annual Field Conference Guidebook, pp. 86–106.
Turowski, J.M., Lague, D., Hovius, N., 2007. Cover effect in bedrock abrasion: a new derivation and its implications for the modeling of bedrock channel morphology. J. Geophys. Res. 112, F04006. https://doi.org/10.1029/2006JF000697.
Venditti, J.G., Kwoll, E., Rennie, C.D., Church, M.A., 2017. Formative flow in bedrock canyons. In: AGU Fall Meeting Abstracts.
Wang, W., Liang, M., Huang, S., 2009. Formation and development of stream potholes in a gorge in Guangdong. J. Geogr. Sci. 19 (1), 118–128. https://doi.org/10.1007/s11442-009-0118.
Williams, G.P., 1978. Bank-full discharge of rivers. Water Resour. Res. 14 (6), 1141–1154. https://doi.org/10.1029/WR014i006p01141.
Wohl, E.E., 2000. Geomorphic effects of floods. In: Inland Flood Hazards: Human, Riparian, and Aquatic Communities. Cambrige University Press, Cambridge, UK, pp. 167–193.
Wohl, E., Ikeda, H., 1997. Experimental simulation of channel incision into a cohesive substrate at varying gradients. Geology 25 (4), 295–298. https://doi.org/10.1130/0091-7613(1997)025<0295:ESOCII>2.3.CO;2.
Wolman, M.G., Miller, J.P., 1960. Magnitude and frequency of forces in geomorphic processes. J. Geol. 68 (1), 54–74. https://doi.org/10.1086/626637.
Yin, D., Peakall, J., Parsons, D., Chen, Z., Averill, H.M., Wignall, P., Best, J., 2016. Bedform genesis in bedrock substrates: Insights into formative processes from a new experimental approach and the importance of suspension-dominated abrasion. Geomorphology. 255, 26–38. https://doi.org/10.1016/j.geomorph.2015.12.008.
Zen, E., Prestegaard, K.L., 1994. Possible hydraulic significance of two kinds of potholes: examples from the paleo-potomac river. Geology 22 (1), 47–50. https://doi.org/10.1130/0091-7613(1994)022<0047:PHSOTK>2.3.CO;2.